iScience

Article

Diversity and evolution of tyrosinase enzymes involved in the adhesive systems of mussels and tubeworms

Graphical abstract

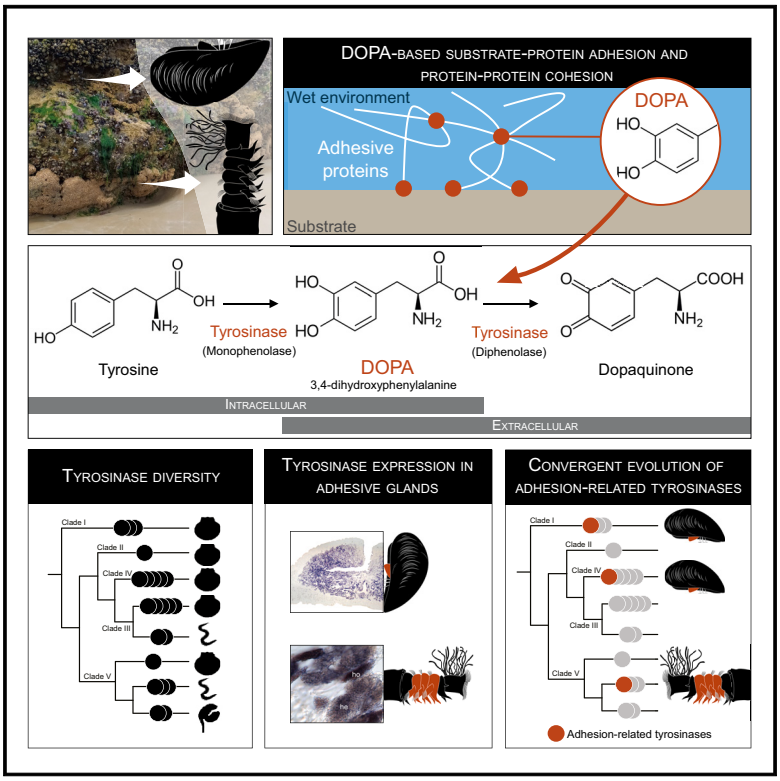

Highlights

- Tyrosinases are multifunctional enzymes playing numerous important roles in metazoans
- We identified tyrosinases involved in adhesive protein maturation in mussels and tubeworms
- Some tyrosinases are gland specific in mussels but not in tubeworms
- The phylogeny of tyrosinases indicates a convergent evolution of the adhesive systems

Authors

Emilie Duthoo, Jérôme Delroisse, Barbara Maldonado, ..., Cécile Van de Weerdt, Matthew J. Harrington, Patrick Flammang

Correspondence

matt.harrington@mcgill.ca (M.J.H.), patrick.flammang@umons.ac.be (P.F.)

In brief

Zoology; Biochemistry; Evolutionary biology; Phylogenetics

Duthoo et al., 2024, iScience 27, 111443
December 20, 2024
https://doi.org/10.1016/j.isci.2024.111443

CellPress

iScience

CellPress
OPEN ACCESS

Article

Diversity and evolution of tyrosinase enzymes involved in the adhesive systems of mussels and tubeworms

Emilie Duthoo,[1] Jérôme Delroisse,[1,2] Barbara Maldonado,[1,3] Fabien Sinot,[1] Cyril Mascolo,[4] Ruddy Wattiez,[4] Pascal Jean Lopez,[5] Cécile Van de Weerdt,[3] Matthew J. Harrington,[6,*] and Patrick Flammang[1,7,*]

[1]Biology of Marine Organisms and Biomimetics Unit, Research Institute for Biosciences, University of Mons, Place du Parc 23, 7000 Mons, Belgium

[2]Laboratory of Cellular and Molecular Immunology, GIGA Institute, University of Liège, 11 avenue de l'hôpital, 4000 Liège, Belgium

[3]Molecular Biomimetic and Protein Engineering Laboratory, GIGA, University of Liège, 11 avenue de l'hôpital, 4000 Liège, Belgium

[4]Laboratory of Proteomics and Microbiology, Research Institute for Biosciences, University of Mons, Place du Parc 23, 7000 Mons, Belgium

[5]UMR Biologie des Organismes et des Ecosystèmes Aquatiques, MNHN/CNRS-7208 Sorbonne Université/IRD-207/UCN /UA, 43 rue Cuvier, 75005 Paris, France

[6]Department of Chemistry, McGill University, 801 Sherbrooke Street West, Montreal, QC H3A 0B8, Canada

[7]Lead contact

*Correspondence: matt.harrington@mcgill.ca (M.J.H.), patrick.flammang@umons.ac.be (P.F.)

https://doi.org/10.1016/j.isci.2024.111443

SUMMARY

Mussels and tubeworms have evolved similar adhesive systems to cope with the hydrodynamics of intertidal environments. Both secrete adhesive proteins rich in DOPA, a post-translationally modified amino acid playing essential roles in their permanent adhesion. DOPA is produced by the hydroxylation of tyrosine residues by tyrosinase enzymes, which can also oxidize it further into dopaquinone. We have compiled a catalog of the tyrosinases potentially involved in the adhesive systems of *Mytilus edulis* and *Sabellaria alveolata*. Some were shown to be expressed in the adhesive glands, with a high gland specificity in mussels but not in tubeworms. The diversity of tyrosinases identified in the two species suggests the coexistence of different enzymatic activities and substrate specificities. However, the exact role of the different enzymes needs to be further investigated. Phylogenetic analyses support the hypothesis of independent expansions and parallel evolution of tyrosinases involved in DOPA-based adhesion in both lineages.

INTRODUCTION

Many marine organisms have evolved diverse attachment strategies to cope with their hydrodynamic environment.[1] In particular, marine invertebrates rely on proteinaceous underwater adhesives for both permanent and temporary attachment to surfaces in the intertidal zone.[2,3] These adhesives are known for their superior strength and durability compared with man-made materials and can therefore provide inspiration for the design and implementation of robust underwater adhesive strategies.[4] Two of the most extensively investigated organisms in this context are mussels and tubeworms (Figures 1A–1C). To attach themselves to rocks, mussels produce a byssus, which consists of a set of protein threads, each connected proximally to the base of the animal's foot (Figure 1B), inside the shell, and ending distally in a flattened plaque sticking to the substratum.[5] Byssal threads are formed by the auto-assembly of proteins secreted by three distinct glands enclosed in the mussel foot: the plaque gland, the core gland, and the cuticle gland.[5,6] To build and expand the tube in which they live, tubeworms of the family Sabellariidae collect mineral particles from their surroundings, dab them with spots of cement, and then add them to the opening of their tube.[7,8] The cement consists mostly of several different proteins produced by two types of parathoracic unicellular glands (cells with homogeneous granules and cells with heterogeneous granules) (Figure 1C).[9,10] The presence of DOPA (3,4-dihydroxy-L-phenylalanine) is a distinctive feature common to proteins identified in the adhesive systems of both mussels and tubeworms.[11–13] This post-translationally modified amino acid fulfills crucial roles in both interfacial adhesive and bulk cohesive interactions within the adhesive secretions.[5,14] DOPA is produced by the post-translational hydroxylation of tyrosine residues of the adhesive proteins by tyrosinase enzymes.[15,16]

Tyrosinases belong to the type-3 copper protein family alongside hemocyanins.[19] These oxygen-transferring copper metalloproteins catalyze the *o*-hydroxylation of monophenols (e.g., tyrosine) into *o*-diphenols (e.g., DOPA) and the further oxidation of *o*-diphenols to *o*-quinones (Figure 1E).[19,20] Consequently, these enzymes exhibit both cresolase (monophenol monooxygenase, EC 1.14.18.1) and catecholase (catechol oxidase, EC 1.10.3.1) activities.[21] Tyrosinases are distributed throughout the Tree of

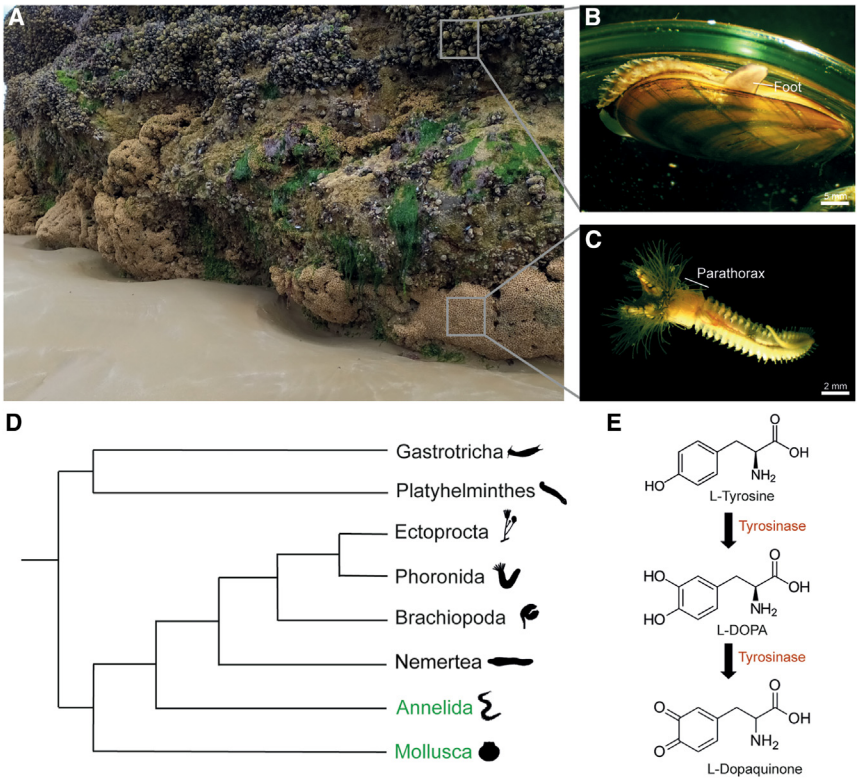

Figure 1. Mussels and tubeworms share a similar DOPA-based adhesion

(A) Intertidal zone with a honeycomb worm reef covered by blue mussels (Douarnenez, France) (Picture courtesy of Alexia Lourtie).

(B and C) *Mytilus edulis* and *Sabellaria alveolata*, respectively.

(D) Phylogenetic position of mussels (Mollusca) and tubeworms (Annelida) (in green) within the Spiralia (based on Laumer et al., 2015[17]).

(E) The possible dual function of tyrosinase enzymes in the maturation of adhesive proteins comprising the modification of tyrosine residues into DOPA and the further oxidation of DOPA into dopaquinone.[18]

Life.[19] They are among the most widespread enzymes in nature as they are key enzymes for pigment synthesis in many organisms.[22] They are also involved in many other biological processes such as shell formation in molluscs[23] or wound healing,[24,25] parasite encapsulation,[26] and cuticle sclerification in insects.[27,28] Regardless of their biological function, all tyrosinases share a common origin traceable to an ancestral tyrosinase gene.[18] Lineage-specific gene duplication events took place during tyrosinase evolution, potentially contributing to functional diversification in specific taxa.[19,29]

Compared to the detailed knowledge available on mussel and tubeworm adhesive proteins, little information exists about the tyrosinases present in the adhesive systems of these organisms. In the mussel *Mytilus edulis*, Waite (1985), and later Hellio and collaborators (2000), reported the partial purification and kinetics of tyrosinases extracted from the foot and the byssus and which displayed a catechol oxidase activity.[30,31] More recently, developments in transcriptomics and proteomics allowed the discovery of new foot- or byssus-specific tyrosinase sequences. Guerette et al. (2013) identified five isoforms from the foot of the green mussel *Perna viridis*, whereas Qin et al. (2016) detected six isoforms in the byssus of *Mytilus coruscus*.[32,33] Their distribution within the foot or the byssus suggests they might have specific substrates and/or functions. In tubeworms, one tyrosinase was identified in *Phragmatopoma californica* and shown to be expressed in the two types of adhesive glands.[10] A later study from the same authors demonstrated that the enzyme was a catechol oxidase that catalyzes the covalent cross-linking of L-DOPA.[34] In two other species, *Phragmatopoma caudata* and *Sabellaria alveolata*, a differential transcriptomic study highlighted 23 tyrosinase transcripts overexpressed in the region of the body enclosing the adhesive glands.[35] Many studies therefore point to an expansion of the tyrosinase repertoire linked to the maturation of adhesive proteins in both mussels and tubeworms.

The adhesive secretions of mussels and tubeworms provide a molecular model for studying the evolution of tyrosinases and the diversification of their functions. Despite belonging to two distinct phyla, mussels and tubeworms are phylogenetically close, both being lophotrochozoans (Figure 1D). Moreover, co-occurring in some intertidal habitats, they are subjected to the same environmental conditions and selective pressures, and their adhesive mechanisms are notably similar, primarily relying on DOPA. Several reviews have hinted at this similarity.[4,11,36,37] However, due to the short and intrinsically disordered nature of the adhesive protein sequences in both mussels and tubeworms, no homology can be traced between them, and they are thought to have evolved independently.[38] Examining the enzymes involved in the maturation process of adhesive proteins, especially tyrosinases, in these two taxa could provide insights into the evolutionary relationships between their adhesive systems. In this study, we investigated the catalog of tyrosinases potentially involved in the maturation of adhesive proteins in the blue mussel *M. edulis* and the honeycomb worm *S. alveolata* by performing proteotranscriptomic analyses. *In situ* hybridization was then used to confirm the expression of these candidate enzymes in adhesive glands, validating their role in bioadhesion. Finally, we conducted phylogenetic analyses to address the question of the evolution and diversification of tyrosinases in these two lineages.

RESULTS

Transcriptomic analyses

The initial phase of this study aimed at identifying enzymes containing a tyrosinase domain that might play a role in adhesive protein maturation in both *M. edulis* and *S. alveolata*. To achieve

this, a mussel foot transcriptome and a honeycomb worm anterior part transcriptome were obtained. Both transcriptomes were generated from 100 bp reads sequenced using the Illumina platform. The raw data comprise 6.1 Gbp for *S. alveolata* and 3.9 Gbp for *M. edulis*. The *M. edulis* dataset contains 173,165 predicted genes, encompassing a total of 152,956,891 nucleotides. The contig N50 is 1,652 nucleotides, with a maximum contig length of 19,275 nucleotides. The *S. alveolata* dataset includes 414,599 predicted genes, amounting to 332,743,778 nucleotides in total. The contig N50 is 1,409 nucleotides, and the maximum contig length is 31,799 nucleotides. The sequence length distribution of the predicted transcripts is shown in Figures S1A and S1B. The completeness of both transcriptome datasets was evaluated using BUSCO (Benchmarking Universal Single-copy Orthologue) analyses on assembled transcripts. Scores were evaluated using the predefined lineage data "Metazoan_odb10". For the *M. edulis*, analyses showed that 92.4% complete BUSCO groups were detected in the gene set. In detail, out of the 954 evaluated BUSCOs from the Metazoan dataset, only 5.2% were fragmented and 2.4% were missing. For *S. alveolata*, the BUSCO analyses indicated that 97.8% complete BUSCO groups were detected with only 2.2% and 0% of fragmented and missing BUSCO groups (Figure S1C). Transcriptome data were then used to search for tyrosinase mRNA sequences using a similarity-based approach. A dataset of tyrosinases comprising mussel byssus (*Mytilus coruscus*,[33] *Perna viridis*[32]) and tubeworm cement (*Phragmatopoma californica*[10]) sequences (see Table S1) was used for local tBLASTn searches in the two transcriptomes to highlight sequences with similarity to these tyrosinases. Candidate matches were then used as queries in a reciprocal BLASTn search against online databases, and only those corresponding to a tyrosinase-like protein as the reciprocal hit were kept as putative candidates. Additionally, after *in silico* translation, short sequences and sequences lacking a tyrosinase domain (cl02830 or pfam00264) were removed.

In the blue mussel, the BLAST searches allowed retrieval of 85 transcripts coding for proteins with tyrosinases as the best reciprocal hit. This list was reduced to 17 candidates when only the longest sequences comprising a tyrosinase domain were considered. Most of the 17 sequences are full-length, except for Medu-TYR2 (comp79852) and Medu-TYR3 (comp74994) that lack the C-terminal region. Eight of these tyrosinases are the closest homologues (BLAST best hits) of the reference tyrosinases from *M. coruscus* and *P. viridis* (Table 1). All these proteins possess a signal peptide indicating they are potentially secreted at the level of the foot, some of them presumably by the byssus-forming glands. Yet, the expression level of the tyrosinase encoding transcripts, expressed as fragments per kilobase of transcript per million mapped reads (FPKM), is on average one to two orders of magnitude lower than that of transcripts coding for mfp-1, mfp-2, and PreCol-NG, three byssal proteins produced by the cuticle, plaque, and core glands, respectively (Table 1).

In the honeycomb worm, a total of 86 transcripts encoding tyrosinase-like enzymes were identified, among which 28 were (almost) full-length and, once translated *in silico*, comprised a tyrosinase domain. For *S. alveolata*, an additional filtering step was implemented based on the differential expression data reported in Buffet et al. (2018).[35] Only transcripts overexpressed in the parathoracic region of the worms were considered, bringing the number of candidates down to 13 (Table 2). In this species too, most of the sequences were full-length, except for Salv-TYR1 (comp274293), which is incomplete in N-term and therefore lacks a signal peptide. Although the sequence of Salv-TYR3, the closest homologue to the catechol oxidase from *P. californica*, appeared to be complete in our transcriptome, no signal peptide could be detected. Similar to mussels, the expression level of mRNAs encoding tyrosinases is much lower than that of mRNAs encoding the cement proteins Sa-1, Sa-2, and Sa-3A/B (Table 2).

Proteomic analyses

We carried out protein analyses on different samples from *M. edulis.* The secretion of byssal threads was induced by injecting KCl at the base of the foot. These freshly secreted threads were collected with fine forceps, and the proteins comprising them were extracted with an 8M urea solution in 5% acetic acid and analyzed by *de novo* peptide sequencing in mass spectrometry (ESI-MS/MS). In addition, mussel feet were dissected and cut in half to separate the foot tip from the basal part. Foot proteins were extracted with 4% sodium dodecyl sulfate (SDS) and were also analyzed by MS/MS after trypsin digestion. By comparing the mass spectrometry results with the foot transcriptome, a total of seven tyrosinases were identified with at least two peptides, with five detected in both the induced threads and foot samples, with a high peptide coverage, and two detected exclusively in the foot samples, but with only three peptides each (Table 1). Medu-TYR1, for example, exhibited the highest peptide coverage, and its corresponding transcript was also the most abundant in the transcriptome compared to other candidates (Table 1). However, the correlation between abundance at the transcript and protein levels does not hold true for the other candidates. Among the tyrosinases identified in foot tissues, two were expressed exclusively in the tip (Medu-TYR8 and 12), two in the basal part (Medu-TYR5 and 10), and three in both parts (Medu-TYR1, 2 and 11). As for the byssal proteins used for comparison, two were detected (mfp-2 and preCol-NG) in all samples, and their distribution in the foot corresponded to their expected expression pattern, only in the tip for mfp-2 and in the basal part of the foot for preCol-NG (Table 1). Due to its tandemly repeated sequence making assembly difficult, Mfp-1 was represented in our transcriptome with two partial transcripts. Only two peptides corresponding to the sequence encoded by one of these transcripts could be detected by mass spectrometry.

In *S. alveolata*, the proteomic analysis was performed on tube fragments constructed by the worms using glass beads. Indeed, in the laboratory, isolated individuals can rebuild their tubes with different materials, including clean glass beads. Freshly constructed tube fragments were collected, and proteins were extracted from the cement dots present on the surface of glass beads using 7M guanidine hydrochloride. Despite these highly denaturing conditions, no protein was detected in mass spectrometry, suggesting that the adhesive secretion might be highly cross-linked and therefore posed challenges for protein extraction.

Table 1. List of tyrosinase sequences identified in the mussel *Mytilus edulis* after proteo-transcriptomic analyses (see text for details)

Sequence name	Clade in phylogenetic tree	Transcript ID	FPKM	Length (aa)	Signal peptide	Number of peptides identified by proteomic analyses			Reciprocal hit tBLASTn	
						BT	DF	PF	Name	Accession number
Tyrosinases										
Medu-TYR1	I	comp83177_c0_seq2	510.1	702	Yes	30	17	17	*M. coruscus* byssal tyrosinase	KX268645
Medu-TYR2	I	comp79852_c1_seq2	59.2	678*	Yes	10	10	2	*M. coruscus* byssal tyrosinase	KX268645
Medu-TYR3	I	comp74994_c0_seq1	8.1	489*	Yes	1	/	/	*M. coruscus* byssal tyrosinase	KX268645
Medu-TYR4	I	comp80529_c1_seq1	32.9	686	Yes	/	/	/	*M. coruscus* byssal tyrosinase	KX268645
Medu-TYR5	I	comp87104_c0_seq11	64.7	805	Yes	/	/	3	*Mizuhopecten yessoensis* tyrosinase	XM_021518068
Medu-TYR6	I	comp75651_c0_seq1	17.83	802	Yes	/	/	/	*Mytilus californianus* uncharacterized LOC127724782	XM_052231853
Medu-TYR7	II	comp83597_c2_seq1	12.6	580	Yes	/	/	/	*M. californianus* uncharacterized LOC127706830	XM_052211537
Medu-TYR8	III	comp66244_c0_seq1	15.0	573	Yes	/	/	/	*M. californianus* tyrosinase-like	XM_052233075
Medu-TYR9	III	comp83819_c0_seq1	34.9	628	Yes	/	/	/	*M. californianus* uncharacterized LOC127706823	XM_052211524
Medu-TYR10	IV	comp85123_c3_seq1	215.0	696	Yes	26	3	12	*M. coruscus* byssal tyrosinase	KP322726
Medu-TYR11	IV	comp76132_c0_seq1	80.9	648	Yes	21	2	8	*M. coruscus* byssal tyrosinase	KP322726
Medu-TYR12	IV	comp83122_c1_seq1	29.9	694	Yes	20	16	/	*M. coruscus* tyrosinase	KP876481
Medu-TYR13	IV	comp72405_c0_seq1	12.1	439	Yes	1	/	/	*M. coruscus* tyrosinase-like	KP757802
Medu-TYR14	IV	comp76510_c0_seq1	1.3	393	Yes	/	/	/	*M. californianus* tyrosinase-like	XM_052215114
Medu-TYR15	IV	comp79670_c1_seq2	192.8	561	Yes	/	/	/	*M. galloprovincialis* catechol oxidase	MG975894
Medu-TYR16	IV	comp83799_c1_seq1	66.0	490	Yes	/	/	/	*M. californianus* tyrosinase-like	XM_052240476
Medu-TYR17	IV	comp84313_c0_seq2	5.0	597	Yes	/	/	/	*M. californianus* tyrosinase-like	XM_052207170
Other representative byssal proteins										
Mfp-1	–	comp48040_c0_seq1	2213.6	100*	No	/	/	/	*M.edulis* gene for polyphenolic adhesive protein	X54422
	–	comp63881_c0_seq2	0.38	165*	No	/	2	/	*Mytilus edulis* clone 21 foot protein 1 (fp-1) mRNA, complete cds	AY845258
Mfp-2	–	comp74249_c0_seq2	4210.2	508	Yes	17	19	/	*M. edulis* clone 7 foot protein 2 (fp-2) mRNA	AY845261
PreCol-NG	–	comp75832_c0_seq1	1594.5	339	Yes	12	/	5	*M. edulis* non-gradient byssal precursor, mRNA	AF414454

Proteins with names in bold are the closest homologues to reference tyrosinases from *M. coruscus* and *P. viridis*. Indicated are the transcript ID form the foot transcriptome, the normalized expression level of the transcripts in the transcriptome (FPKM), the protein length in amino acid (with asterisks indicating incomplete sequences), the presence of a signal peptide, the peptide coverage of the translated transcripts from the MS-MS analysis (number of detected peptides in induced byssal threads [BT], distal foot tissues [DF] and proximal foot tissues [PF]), the position in the phylogenetic tree (Figure 3), and top reciprocal BLAST hit. Three byssal proteins representative of the cuticle (Mfp-1), plaque (Mfp-2), and core (PreCol-NG) glands are included for comparison.

Table 2. List of tyrosinase sequences identified in the tubeworm *Sabellaria alveolata* after transcriptomic analyses (see text for details)

Name	Clade in phylogenetic tree	Transcript ID	FPKM	Differential expression	Length (aa)	Signal peptide	Reciprocal hit tBLASTn	
							Name	Accession number
Tyrosinases								
Salv-TYR1	V	Comp274293_c0_seq4	6.1	−7.29	470*	No	*Phragmatopoma californica* tyrosinase-like protein	JN607213.2
Salv-TYR2	V	Comp275725_c0_seq1	8.1	−11.85	476	Yes	*Phragmatopoma californica* tyrosinase-like protein	JN607213.2
Salv-TYR3	V	Comp278284_c0_seq2	9.2	−8.84	432	No	*Phragmatopoma californica* tyrosinase-like protein	JN607213.2
Salv-TYR4	V	Comp264814_c0_seq1	1.7	−4.89	434	Yes	*Phragmatopoma californica* tyrosinase-like protein	JN607213.2
Salv-TYR5	V	comp276298_c0_seq1	82.3	−4.43	477	Yes	*Phragmatopoma californica* tyrosinase-like protein	JN607213.2
Salv-TYR6	V	comp277654_c0_seq1	97.5	−4.39	458	Yes	*Phragmatopoma californica* tyrosinase-like protein	JN607213.2
Salv-TYR7	V	comp239180_c0_seq1	130	−4.44	489	Yes	*Phragmatopoma californica* tyrosinase-like protein	JN607213.2
Salv-TYR8	V	comp275276_c0_seq1	27.1	−3.86	515	Yes	*Phragmatopoma californica* tyrosinase-like protein	JN607213.2
Salv-TYR9	V	comp279307_c0_seq1	52	−4.42	471	Yes	*Phragmatopoma californica* tyrosinase-like protein	JN607213.2
Salv-TYR10	V	comp276771_c7_seq1	136.7	−4.21	450	Yes	*Phragmatopoma californica* tyrosinase-like protein	JN607213.2
Salv-TYR11	V	comp269290_c0_seq1	24.3	−7.23	515	Yes	*Lingula anatina* putative tyrosinase-like	XM_024075990.1
Salv-TYR12	V	comp280500_c0_seq2	8.3	−4.07	504	Yes	*Phragmatopoma californica* tyrosinase-like protein	JN607213.2
Salv-TYR13	V	comp273963_c1_seq5	141.7	−4.08	402	Yes	*Lingula anatina* putative tyrosinase-like	XM_013539498.1
Other representative cement proteins								
Sa-1	–	comp225468_c0_seq2	30403	−4.25	112	Yes	NA	–
Sa-2	–	comp271660_c3_seq1	23866.7	−3.95	102	Yes	NA	–
Sa-3a	–	comp271458_c0_seq5	1061.7	−4.52	298	Yes	NA	–
Sa-3b	–	comp267107_c0_seq3	1867.6	−4.96	213	Yes	*Sabellaria alveolata* mRNA for cement precursor protein 3B	HE599639.1

The protein with the name in bold is the closest homologue to the reference tyrosinase from *P. californica*. Indicated are the transcript ID from the transcriptome of the anterior part of the worm, the normalized expression level of the transcript in the transcriptome (FPKM), the differential expression of the transcript between the parathoracic part of the worm and the rest of its body (log2-FoldChange reported in Buffet et al., 2018[35]), the protein length in amino acid (with asterisks indicating incomplete sequences), the presence of a signal peptide, the position in the phylogenetic tree (Figure 3), and the top reciprocal BLAST hit. Four cement proteins are included for comparison.

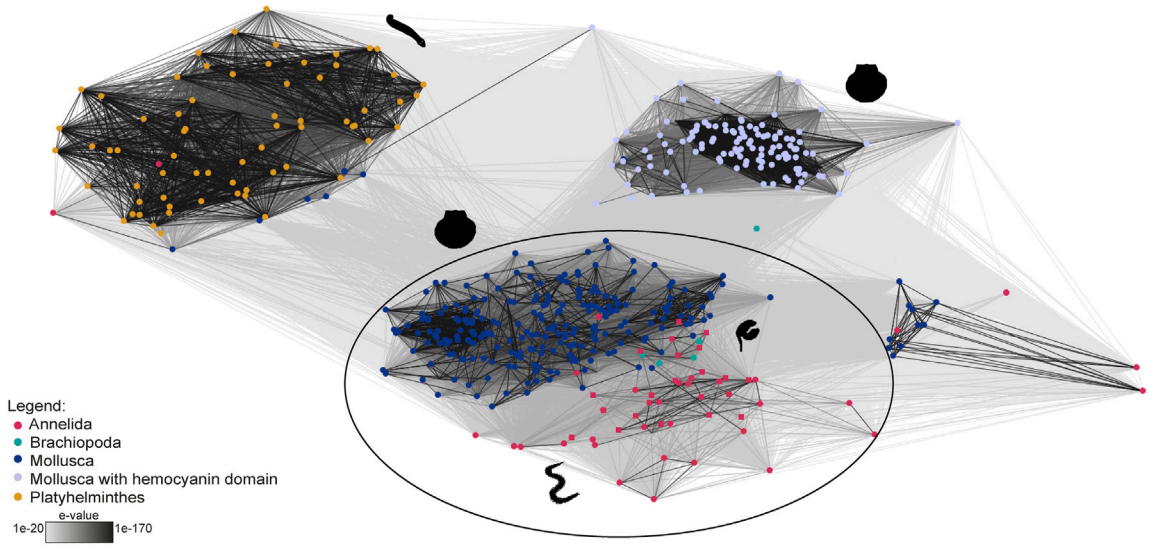

Figure 2. Cluster analysis of tyrosinase sequences from Spiralia

Sequence-similarity-based clustering approach based on BLASTp e-values with the tyrosinase sequences identified in the present work and all the spiralian sequences containing a pfam00264 domain retrieved from the NCBI database. This analysis shows that the different phyla tend to cluster together. The sequences circled were selected for phylogenetic analyses.

Phylogenetic analyses

To gain a comprehensive understanding of the relationships between tyrosinases, we investigated protein sequences containing the tyrosinase domain (pfam00264) from various spiralian species. These sequences were retrieved from the NCBI database. They include 30 proteins from Annelida, 8 from Brachiopoda, 375 from Mollusca, and 63 from Platyhelminthes. Additionally, we incorporated sequences obtained through the proteo-transcriptomic analyses of our two model species, specifically 20 predicted proteins from *M. edulis* (3 sequences found in the mantle were added to the 17 previously identified) and 28 from *S. alveolata* (Tables 1 and 2) (Table S1). A sequence-similarity-based clustering analysis was carried out using CLANS[39] to explore potential similarities between all these tyrosinases. An all-against-all BLASTp was conducted using the scoring matrix BLOSUM62, and linkage clustering was performed with a maximum e-value of $1E^{-20}$ to identify coherent clusters. The clustering was initially performed in three dimensions and then projected into two dimensions to generate the illustration shown in Figure 2. The darker connections between the dots indicate higher similarity between the proteins based on the BLASTp e-values.[40]

The CLANS analysis revealed that spiralian tyrosinases form several clearly distinct clusters, each comprising sequences that share a high similarity among them as evidenced by the low e-values associated to the lines connecting them (Figure 2). All the tyrosinase sequences from each phylum are generally grouped together, although a few isolated dots are noticeable, usually corresponding to very short (partial) sequences or very long sequences (>3,000 amino acids) comprising additional domains (e.g., kielin/chordin-like domain). The phylum Mollusca is an exception as its sequences were divided into two clusters: one comprising sequences with only a tyrosinase domain and one consisting of sequences containing both a tyrosinase (pfam00264) and an hemocyanin domain (pfam14830). Hemocyanins are extracellular proteins involved in oxygen transport and are found in the phyla Arthropoda and Mollusca.[41,42] Previous studies have demonstrated that both hemocyanins and tyrosinases belong to the type 3 copper protein family and share a common ancestor.[43,44] However, structural modifications at the binuclear copper active site underlie the divergent evolution of tyrosinase and hemocyanin functions.[19] This functional divergence may explain why all the Mollusca sequences are not grouped in the same cluster.

In the CLANS analysis, tyrosinase sequences from Platyhelminthes form a well-separated cluster, whereas those from Lophotrochozoa (Brachiopoda, Annelida, and Mollusca) are grouped together (Figure 2). To delve deeper into their evolutionary relationships, the 312 tyrosinase protein sequences from the lophotrochozoan supercluster were subjected to a phylogenetic analysis using molluscan hemocyanins as outgroup (Figures 3 and S2). On the phylogenetic tree generated, five main clades (numbered from I to V on Figure 3) can be distinguished. Clades I to IV group together the sequences from molluscs: clades I, II, and IV contain only tyrosinases from bivalves, whereas clade III includes sequences from all classes of molluscs, from gastropods to cephalopods. Clade V contains a few oyster tyrosinase sequences (Bivalvia, Ostreoida) but comprise mostly non-molluscan sequences. Most of the sequences from the phylum Annelida are grouped with those from Brachiopoda in this clade, except some of the sequences from the polychaete *Owenia fusiformis* (Delle Chiaje, 1844) that are in clade III. The reference byssal tyrosinase sequences from the mytilidae *M. coruscus* and *P. viridis*, as well as their closest homologues from *M. edulis* (Table 1) are localized either in cluster I (e.g., Medu-TYR1 to 4; Figure 3) or in cluster IV

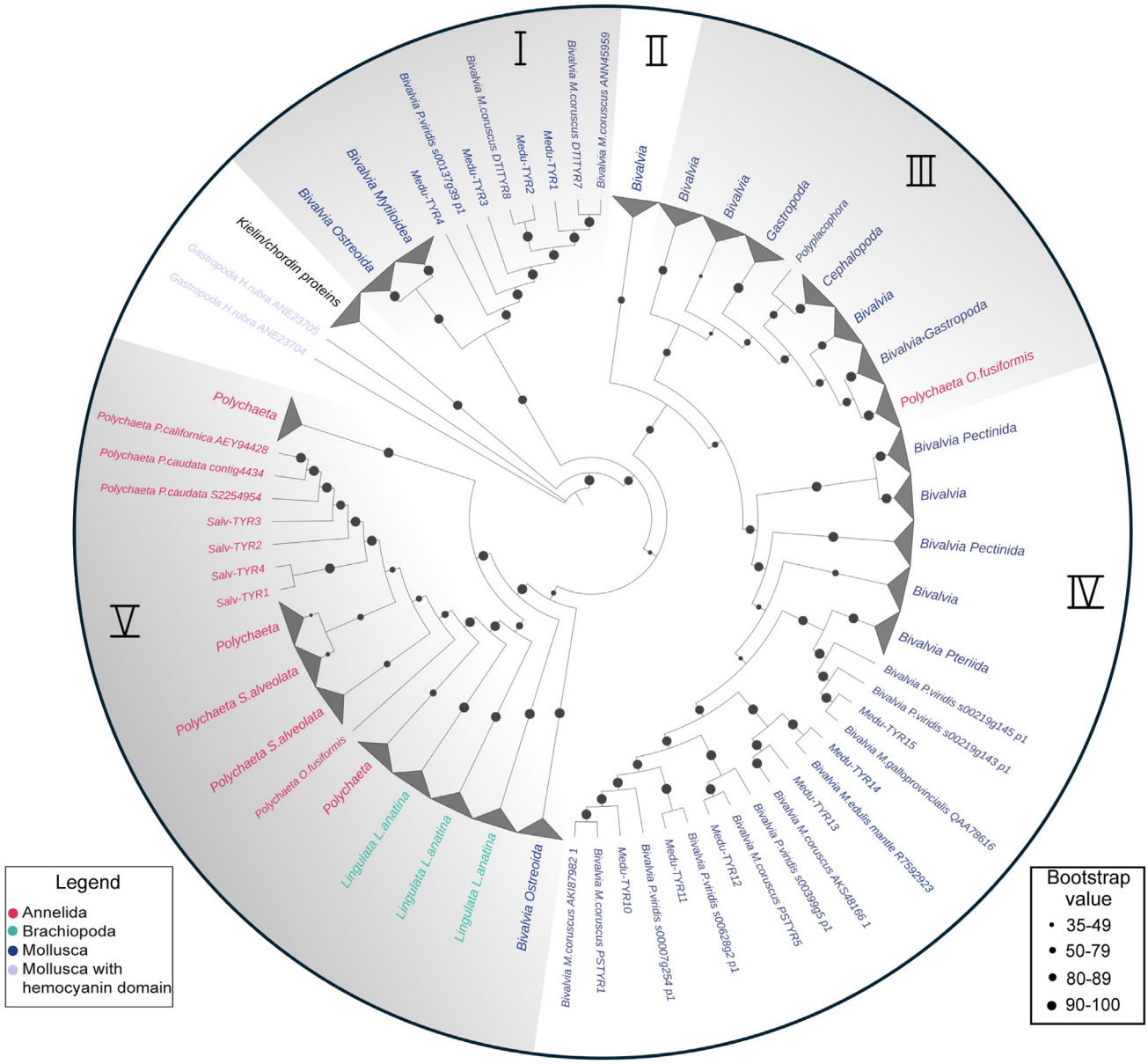

Figure 3. Evolution of tyrosinases in Lophotrochozoa

Maximum likelihood phylogenetic tree showing the distribution of tyrosinase sequences, based on circled sequences selected in the CLANS analysis. The sequences are distributed among five main clades, numbered I to V. The reference byssal tyrosinase sequences from *M. coruscus* and *P. viridis* and their orthologues in *M. edulis* (Table 1) are localized in clusters I and IV, whereas the reference cement tyrosinase from *P. californica* and all sequences from *S. alveolata* (Table 2) are in cluster V. The bootstrap values are shown in the legend in the box. See also Figure S2 for the corresponding detailed tree.

(Medu-TYR10 to 15; Figure 3). However, a few of the sequences shortlisted in the blue mussel are also present in clades II and III (Table 1). The reference cement tyrosinase from *P. californica* and all the sequences from *S. alveolata* are in cluster V. It should be noted that the phylogenetic tree generated from these analyses showed low support for some nodes (Figure 3), likely due to the high level of conservation of residues surrounding the copper-binding sites and globally the short protein-based alignment. Similar results have been observed in previous studies.[35,45]

In situ hybridization experiments

To further investigate the role of the identified enzymes in adhesive protein maturation, the localization of their coding mRNAs in the tissues was determined using *in situ* hybridization (ISH). DIG-labeled RNA probes were designed based on sequences retrieved from the transcriptomes and used on tissue sections from both mussels and honeycomb worms, as well as on whole-mount preparations of the mussel's feet, to determine whether the tyrosinases are expressed in the adhesive-producing gland cells or in other cell

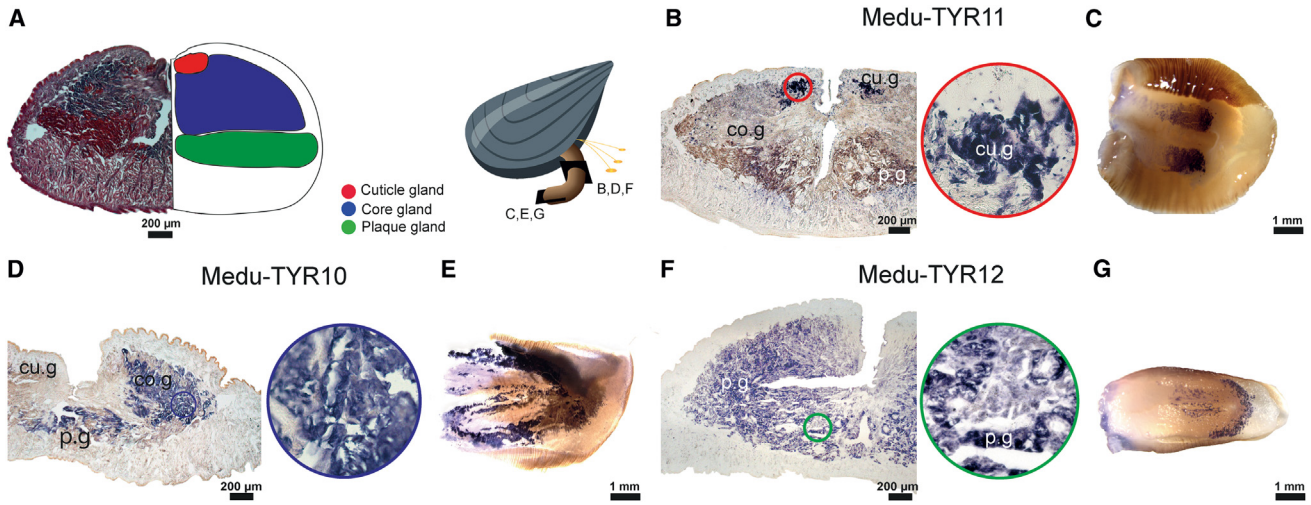

Figure 4. Examples of the expression patterns of selected tyrosinase transcripts in the foot of *Mytilus edulis*

(A) Illustration showing both a transverse histological section of a foot stained with Heidenhain's azan stain (left) and a diagram with the arrangement of the different glands in the foot tissues (right).

(B–G) Section (B, D, F) and whole-mount (C, E, G) *in situ* hybridization of the mRNAs coding for three tyrosinase candidates. Insets in circles show a zoom on the labeled gland. cu.g, cuticle gland; co.g, core gland; p.g, plaque gland. See also Figures S3 and S4 for controls and other transcripts.

types. Controls were performed using sense RNA probes, as well as without probes or without antibody (Figure S3).

In the case of the blue mussel, we selected tyrosinase sequences showing the highest similarity to the reference sequences and/or coding for proteins detected with a minimum of two peptides in the induced byssal threads by MS/MS analyses. This corresponds to nine candidates: Medu-TYR1 to 5, Medu-TYR10 to 12, and Medu-TYR15 (Table 1). *In situ* hybridization was performed on the entire foot cut open in two halves along the central frontal plane (whole-mount; see Figure 4) but also on several transverse sections through the foot to make sure to visualize all specific foot glands, namely the core, cuticle, and plaque glands. For each section processed for ISH, a directly consecutive section was stained with Heidenhain's azan to validate the identification of the glands. The results of the ISH experiments are illustrated in Figures 4 and S4. Among the nine candidates, one was found to be exclusively localized in the plaque gland (Medu-TYR12), one in the core gland (Medu-TYR10), and one in the cuticle gland (Medu-TYR11). On the other hand, five candidates were expressed in at least two glands: both the plaque and the cuticle glands (Medu-TYR4 and 15), both the plaque and core glands (Medu-TYR2 and 5), or both core and cuticle glands (Medu-TYR1). No probe could be produced for the candidate Medu-TYR3.

For the honeycomb worm, four transcripts were selected: those exhibiting the highest similarity to the reference sequence from *P. californica* (Figure 3), among which three were also the most highly differentially expressed in the parathoracic region of the worm (Table 2). The four tyrosinase candidates (Salv-TYR1 to 4) were exclusively expressed in the cement glands (Figure 5). Moreover, they were all expressed within both cells with heterogeneous granules and cells with homogeneous granules (Figure 5). The two types of granules can easily be distinguished at high magnification.

DISCUSSION

Diversity of tyrosinases potentially involved in adhesive protein maturation

Various marine invertebrates rely on quinone-tanned biomaterials as durable glues or protective varnishes.[46] Two well-studied examples of such materials are the byssus produced by mussels and the cement secreted by tube-building worms.[46] These materials contain a catechol known as DOPA, or 3,4-dihydroxyphenylalanine, a modified amino acid that is widely present in nature. DOPA is essential for bonding with the substrate and providing cohesive cross-links within the adhesive materials of these organisms. The enzymes responsible for its production are the tyrosinases that play a crucial role in various biological functions. Although DOPA has been extensively studied in marine adhesion, the specific enzymes responsible for its production are still not well understood. However, several studies have highlighted the fact that not one but several tyrosinases may be involved in the maturation of adhesive proteins in a single organism.[32,33,35] In this study, our first objective was to identify the tyrosinase sequences involved in the adhesive systems of mussels and tubeworms by comparing a set of reference sequences known to be present in the adhesive secretions of some species with the transcriptomes of our two model species, the blue mussel *M. edulis* and the honeycomb worm *S. alveolata*. For both species, more than 80 different tyrosinase-like sequences were retrieved by the BLAST searches, but these numbers were greatly reduced when only (almost) full-length proteins with a tyrosinase domain were considered. Moreover, differential expression, mass spectrometry analyses, and *in situ* hybridization experiments were used to pinpoint the candidate expressed in adhesive glands and secreted.

In the blue mussel, 17 candidates were identified by the *in silico* analyses, among which seven were shown to be present in

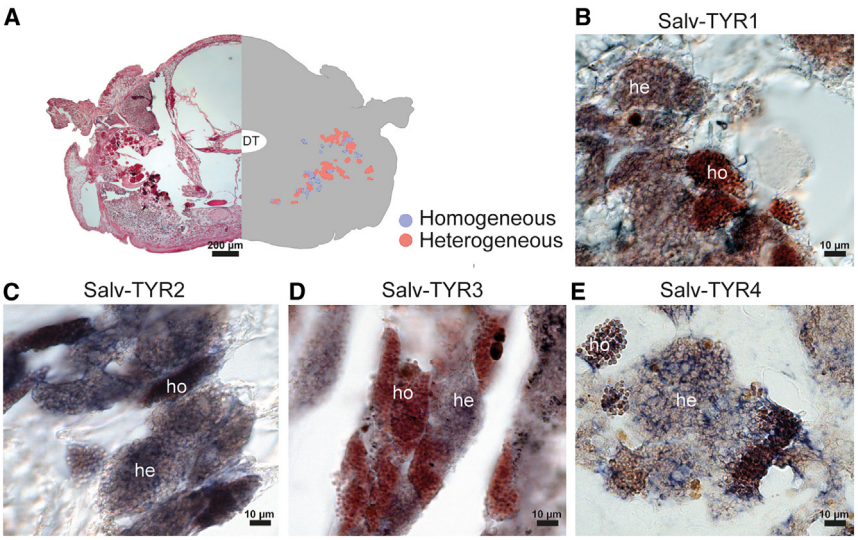

Figure 5. Expression patterns of selected tyrosinase transcripts in the parathoracic region of *Sabellaria alveolata*

(A) Illustration showing both a transverse section of the parathoracic part stained with Heidenhain's azan stain (left) and a diagram showing the arrangement of the cement glands (right).

(B–E) *In situ* hybridization of the mRNAs coding for four tyrosinase candidates. DT, digestive tract; he, cement gland with heterogeneous granules; ho, cement gland with homogeneous granules. See also Figure S3 for controls.

the byssus and/or in the foot tissues by mass spectrometry analyses. In particular, five tyrosinases were detected in induced byssal threads with a high peptide coverage (Medu-TYR1 and 2 and Medu-TYR10 to 12). The mRNAs coding for these five proteins, but also those coding for three other candidates sharing high homology with reference tyrosinases from *M. coruscus* and *P. viridis*, were localized in the foot glands. Two patterns of expression were observed: three candidates (Medu-TYR10 to 12) are each specific in a single gland type, whereas the other five (Medu-TYR1, 2, 4, 5, and 15) have been localized in different glands (Figure 6). The gland-specific mRNA expression of these different tyrosinases corresponds to the localization of the corresponding protein in the foot (distal half, proximal half, or both) for candidates that have been detected in mass spectrometry (Table 1; Figure 6). It also matches the distribution of their homologues within the byssus of *M. coruscus*. For instance, Medu-TYR12, whose mRNA is specifically expressed in the plaque gland, is the closest homologue to a tyrosinase-like protein (encoded by cDNA KP876481; Table 1) identified in the byssal plaque in *M. coruscus*.[33] It is not surprising to find tyrosinases in the three different foot glands involved in byssal threads synthesis as they all produce DOPA-containing proteins (Figure 6).[5] The plaque gland is known to contain more than 10 different proteins,[47] including mfp-3 and -5 that are the byssal proteins with the highest DOPA content (20 and 30 mol %, respectively).[48,49] The cuticle gland produces mfp-1, which contains 15 mol % of DOPA, as well as a handful of other, less-characterized proteins.[47,50] Finally, the preCols and thread matrix proteins secreted by the core gland also contain DOPA, although in lower amounts.[51,52]

In the honeycomb worm, 28 candidate tyrosinase transcripts were retrieved from the transcriptomic analysis. The comparison of these sequences with the differential transcriptome of Buffet et al. (2018)[35] for the same species allowed us to reduce the list to 13 candidates. These transcripts are highly overexpressed in the parathorax, the region of the worm containing the cement glands. A proteomic analysis was conducted on tubes reconstructed by the worm using glass beads but, unfortunately, no tyrosinase or cement protein was detected, suggesting that the proteins could not be extracted from the cement spots binding the beads. Four transcripts, among the most differentially expressed and showing the highest homology with the cDNA encoding the reference tyrosinase from the sandcastle worm *P. californica* (JN607213.2), were selected for localization by *in situ* hybridization. These tyrosinase mRNAs were expressed in both types of unicellular cement glands, the cells with homogeneous granules and the cells with heterogeneous granules (Figure 6), similarly to what was observed in *P. californica*.[10] There was therefore no gland specificity for the four candidates we selected. In *P. californica*, at least two adhesive proteins, Pc-1 and Pc-2, are known to contain DOPA (about 10% and 7%, respectively[53]). The former is produced by cement glands with heterogeneous granules and the latter by glands with homogeneous granules.[10] Their homologues, Sa-1 and Sa-2, have been identified in *S. alveolata*,[9] and preliminary results suggest that their distribution in the cement glands corresponds to the one in *P. californica* (unpublished data). Thus, in the honeycomb worm too, each type of cement gland would produce at least one DOPA-rich protein, which would explain the expression of tyrosinases in both glands (Figure 6).

Although the high diversity of tyrosinase candidates in both model species is suggestive of a variety of functions, linking their sequences with their different functionalities (monooxygenase vs. oxidase) may prove difficult. Tyrosinases and catechol oxidases share a very similar active site architecture in which three distinct oxidation states have been identified, oxy-, deoxy-, and met-states, based on the structure of the bicopper structure of the active center.[21] Transitions from one state to another lead to the molecular mechanisms involved in the monophenolase or diphenolase catalytic activity.[21] However, some enzymes appear to show only the oxidase activity.[54] Moreover, although the active site of tyrosinases is highly conserved, variations exist in their sequences, size, glycosylation, and activation.[55] To date, the structural motifs responsible for the different activities remain elusive.[54] Only homology with enzymes of known function or expression pattern could therefore be used to investigate the function of the new tyrosinase candidates from *M. edulis* and *S. alveolata*.

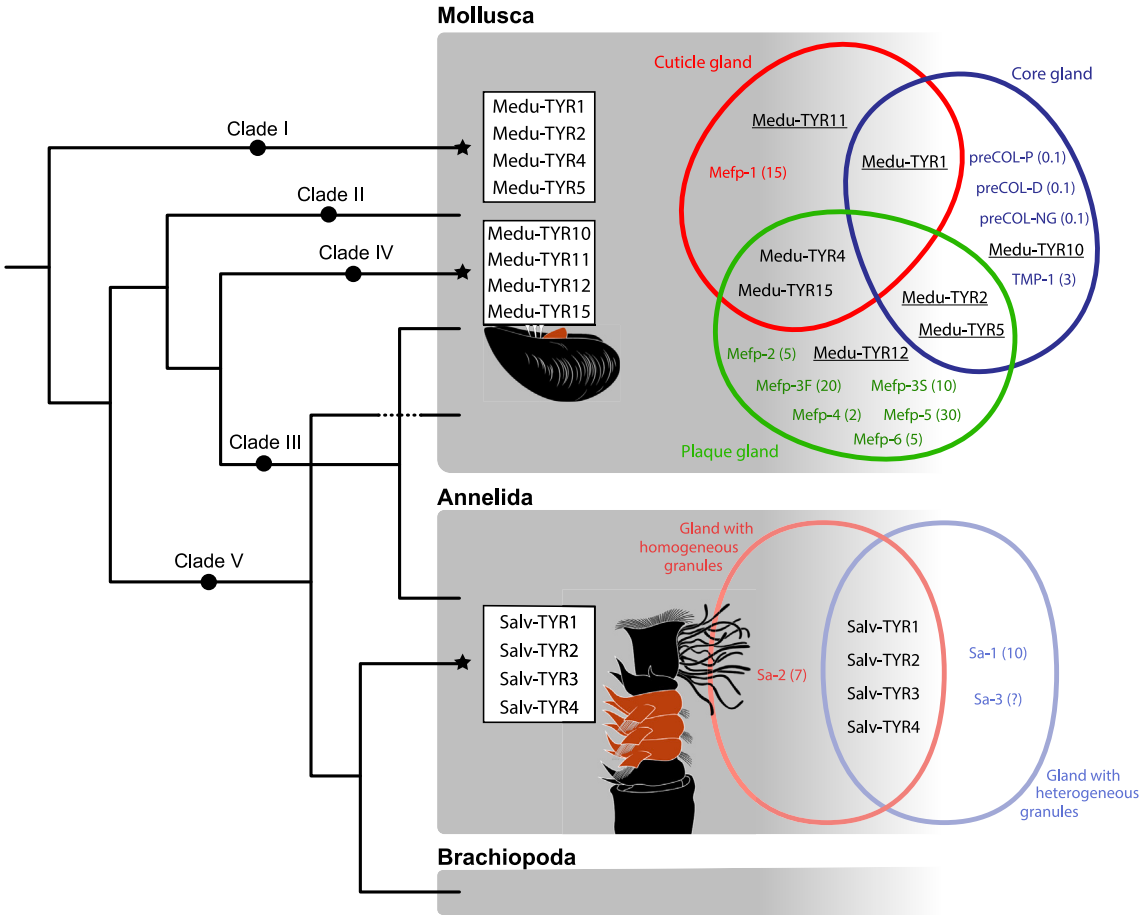

Figure 6. Tyrosinases involved in the adhesive systems of the mussel *Mytilus edulis* and the tubeworm *Sabellaria alveolata*

Simplified tyrosinase phylogenetic tree in which stars indicate the clades comprising enzymes expressed in adhesive glands. The gland specificity of each tyrosinase, as highlighted by *in situ* hybridization experiments, is illustrated on the right. In the mussel, the ISH localization of several candidates (underlined) is supported by mass spectrometry data even though the experimental protocol used (foot distal part vs. foot proximal part) does not allow a precise gland assignment. The main adhesive proteins produced by the different glands have been included, as well as their DOPA content in brackets, expressed in mol % (data from different species[5,53]).

In mussels, DOPA plays important interfacial adhesive and bulk cohesive roles during byssus fabrication.[5,56] Priemel et al. (2020)[16] have identified two distinct DOPA-based cross-linking pathways, one achieved by oxidative covalent cross-linking and the other by the formation of metal coordination interactions under reducing conditions. The former takes place in the thread core, whereas the latter occurs in the cuticle, plaque foam, and plaque-surface interface.[16] In the core gland, preCol-D was shown to possess several DOPA residues at the N-terminus,[51] which, after secretion, are oxidized into dopaquinone for covalent cross-link formation.[16] It is therefore tempting to postulate that the core gland-specific tyrosinase, Medu-TYR10, which is also one of the most highly expressed, could have a catechol oxidase activity. A catechol oxidase was extracted from the foot and byssus of *M. edulis* by Waite (1985),[30] but it is not possible to link it to any of our candidates as no sequence was reported. On the other hand, the DOPA-rich proteins from the cuticle and plaque glands should be prevented from oxidation after secretion to promote intermolecular DOPA-metal coordinated bonds.[16,57] This is possible thanks to a locally low pH and the presence of reducing conditions, usually provided by the sulfhydryl groups of cysteine-rich proteins such as mfp-6.[58] Based on this reasoning, Medu-TYR11 (cuticle gland) and Medu-TYR12 (plaque gland) should only display a monophenolase activity. Unexpectedly, Medu-TYR15, whose corresponding transcript is expressed in both the plaque and cuticle glands, is the closest homologue to a catechol oxidase from *Mytilus galloprovincialis* (Table 1). This catechol oxidase, when expressed recombinantly in bacteria, showed no catalytic activity but instead exhibited a thiol-dependent antioxidant activity suppressing DOPA oxidation.[59] However, Medu-TYR15 was not detected in the byssus or the foot by our proteomic analyses.

In tubeworms, it was demonstrated that the tyrosinase identified in *P. californica* catalyzes only catechol oxidation. This observation was made through substrates and inhibitors profiling on the isolated secretory granules and secreted cement.[34] As Salv-TYR1 to 4 are close homologues to this catechol oxidase and display the same expression pattern in both cement glands, it is likely

that they would also show a diphenolase activity. In *P. californica*, the oxidation of DOPA to dopaquinone leads to the formation of cysteinyl-DOPA covalent cross-links within the cement.[60]

Evolution of tyrosinases in Lophotrochozoa

The high number and diversity of tyrosinases identified in *M. edulis* and *P. californica* prompted us to examine the phylogenetic relationship they have together and with other lophotrochozoan tyrosinases.

Firstly, we built a cluster map of all spiralian sequences containing a tyrosinase domain retrieved from the NCBI nr database. Tyrosinase sequences from Platyhelminthes formed a cluster clearly separated from another large cluster comprising sequences from Brachiopoda, Annelida, and Mollusca. This reflects the evolution of type-3 copper proteins in animals in which three ancestral subclasses (α, β, and γ) have been described, with differential losses or expansions of one or more of these subclasses in specific phyla.[19] Platyhelminthes possess γ-subclass, transmembrane tyrosinases, whereas the three other phyla possess α-subclass, secreted tyrosinases.[19] Molluscan hemocyanins also belong to the α-subclass[19] but form a well-separated cluster compared to tyrosinases.

Secondly, a phylogenetic tree was constructed to examine the relationships between lophotrochozoan tyrosinases, using molluscan hemocyanins as the outgroup. The tyrosinase tree is fairly complex, with five main clades that do not necessarily reflect the main taxonomic groups. Mollusc, annelid, and brachiopod tyrosinases appear to be paraphyletic, and their sequence variation would not be solely influenced by the evolutionary distance between lineages. Indeed, three of the five clades in the tree we generated (clades I, II, and IV) contain exclusively sequences from bivalves, whereas the other two clades (III and V) gather sequences from different phyla or mollusc classes. In their study about the evolution of the tyrosinase gene family in bivalve molluscs, Aguilera et al. (2014)[45] reported that tyrosinase sequences were separated into two clades: an ancestral clade (A) comprising tyrosinases from all mollusc classes and a bivalve-specific clade (B). Based on the sequences shared by the two studies, our clades I, II, III, and V would correspond to their clade A and our clade IV to their clade B. The different tree topology we obtained could be linked to the inclusion of annelid and brachiopod sequences in our tree, a different trimming of the sequences, or a different rooting of the tree. It should also be noted some of the basal nodes in our tree are poorly supported.

The high number of transcripts obtained during our *in silico* analyses supports the hypothesis that the tyrosinase gene family has undergone large independent expansions in bivalve molluscs[45] as well as sabellariid polychaetes.[35] This apparently also includes tyrosinases potentially involved in the maturation of adhesive proteins, with six and four enzymes identified in *M. edulis* and *S. alveolata*, respectively, as shown by proteomic data and/or *in situ* hybridization results (Figure 6). Mussel byssus and tubeworm cement tyrosinase sequences are separated in distinct clusters. This suggests an independent functional evolution of tyrosinases involved in the maturation of bioadhesives in these two lineages. Interestingly, the mussel tyrosinases are also distributed in two different clusters (I and IV), and enzymes from both clusters are co-expressed in the same foot gland. The identification of byssal tyrosinases in these two different clusters is congruent with the results of Aguilera et al. (2014),[45] indicating an early gene duplication in bivalve evolution. These genes would then have undergone further independent duplication and divergence to acquire new gene functions.

Implication for the development of biomimetic adhesives

Marine adhesives display impressive performances in their natural context and, therewith, the potential to inspire novel adhesives working in fluid environments, including the human body.[2] Marine adhesive proteins have therefore been exploited to produce increasingly complex biomaterials with added functionalities, such as wearable electronics or drug delivery systems.[61] Many of these materials utilize recombinant proteins, which are generally seen as the closest mimics of marine adhesive proteins and can be synthesized in sufficient quantities for incorporation in biomaterials.[62] Recombinant DNA technology also comes with the possibility to alter and rearrange protein sequences by genetic engineering to create new truncated or chimeric proteins.

Because the mussel's byssus is the best-characterized marine bioadhesive, it is in these organisms that most of the recombinant adhesive proteins have been produced.[63,64] Many mfps from the cuticle and plaque glands, as well as the preCols from the core gland, have been produced in heterologous host cells such as bacteria or yeasts.[63] However, in all these recombinant proteins, important native post-translational modifications are missing, such as the hydroxylation of tyrosine residues into DOPA. Protocols have thus been developed for the *in vitro* conversion of tyrosine residues to DOPA utilizing a mushroom tyrosinase, but they exhibit low modification yields that can limit underwater adhesion.[65,66] In another approach, a co-expression system was used in bacteria, with the concomitant production of mfps and bacterial or mushroom tyrosinases with a dual vector system.[67,68] The *in vivo* modification efficiency was higher than that *in vitro*, leading to an increased adhesive strength.[67] Under the assumption that tyrosinases produced in specific glands have evolved to specifically modify the DOPA-containing proteins synthesized and stored in that gland, we hypothesize that using the appropriate tyrosinase to target and modify a given recombinant protein might give improved DOPA modification yield and thus materials performance. For example, one could co-express a mussel adhesive protein with the specific mussel tyrosinase expressed in the same gland (e.g., mfp-3 or mfp-5 with Medu-TYR12). Before this can become a reality, however, the tyrosinases identified in the present study need to be produced recombinantly, better characterized and their function confirmed by *in vitro* assays.

Conclusion

Honeycomb worms and blue mussels are frequently found together in the intertidal zone, where they encounter similar environmental challenges. Both organisms rely on a DOPA-based adhesive system, and our study has identified a catalog of tyrosinase enzymes involved in the maturation of adhesive proteins in *M. edulis* and *S. alveolata*. The diversity of tyrosinases highlighted in the two species suggests the coexistence of different

functions (monophenol monooxygenase or catechol oxidase activity) or different substrate specificities. However, the exact role of the different enzymes needs to be further investigated. Phylogenetic analyses support the hypothesis of independent expansion and parallel evolution of tyrosinases involved in adhesive protein maturation in both lineages, supporting the convergent evolution of their DOPA-based adhesion. These results contribute to our understanding of the molecular basis of adhesion mechanisms in marine organisms but also pave the way toward the use of specific tyrosinases in development of biomimetic adhesives.

Limitations of the study

Our study presents certain limitations that should be highlighted. We did not explore the complete tyrosinase repertoire of the blue mussel (*M. edulis*) and the honeycomb tubeworm (*S. alveolata*) based, for example, on complete chromosome-scale genomes. Rather, using a set of reference tyrosinase sequences from the literature, we specifically focused on tyrosinase sequences retrieved from a foot transcriptome for the mussel and from a parathoracic region transcriptome for the tubeworm—tissues relevant for the material formation processes in question. Although we identified several candidates expressed in adhesive-secreting tissues, we might have missed species-specific or highly derived tyrosinases using this approach. Moreover, additional *in situ* hybridization experiments could be conducted to highlight the expression patterns of other candidates from our list. Although we provided evidence of tyrosinase production and secretion at the protein level through mass spectrometry analyses, the use of specific antibodies could further validate the expression profiles of the identified proteins. Another limitation is that our study does not address the functional roles of the tyrosinases investigated. *In vitro* functional characterization of the tyrosinases of interest will be crucial for validating their specific molecular functions and could potentially lead to the emergence of new avenues in bio-inspired research and biomaterial development.

RESOURCE AVAILABILITY

Lead contact

Further information and requests should be directed to the lead contact, Patrick Flammang (Patrick.Flammang@umons.ac.be).

Materials availability

This study did not generate unique materials.

Data and code availability

- The RNAseq data can be accessed through NCBI Sequence Read Archive (NCBI SRA: SSR29446349 and NCBI SRA: SSR29446350 for *M. edulis* and *S. alveolata*, respectively).
- This article does not report original code.
- Other data will be made available upon reasonable request by the lead contact.

ACKNOWLEDGMENTS

We thank Dominique Baiwir from the GIGA Proteomics Facility (ULiège, Belgium) for the mass spectrometry-based analyses conducted on mussel feet, as well as Antoine Flandroit, Nathan Puozzo, and Paolo Rosa for their help with microphotography and figures. We also acknowledge the support of the Research Institute for Biosciences of UMONS. This work was supported by the Fund for Scientific Research of Belgium (F.R.S.-FNRS) through (1) a FRIA doctoral fellowship to E.D., (2) a CR postdoctoral fellowship to B.M., and (3) a research project (PDR T.0088.20). P.J.L. would also like to thank the Labex DRIIHM, the French program "Investissements d'Avenir" (ANR-11-LABX-0010), which is managed by the French National Research Agency (ANR). J.D. is financially supported by a F.R.S.-FNRS research project (PDR T.0169.20) granted to UMONS and ULiège. P.F. is Research Director of the F.R.S.-FNRS.

AUTHOR CONTRIBUTIONS

Conceptualization, E.D., J.D., M.J.H., and P.F.; methodology, E.D., C.M., and J.D.; investigation, E.D., B.M., F.S., and J.D.; writing—original draft, E.D., J.D., and P.F.; writing—review & editing, all co-authors; funding acquisition, P.J.L. and P.F.; resources, P.J.L. and R.W.; supervision, C.V.W., M.J.H., and P.F.

DECLARATION OF INTERESTS

The authors declare no competing interests.

STAR★METHODS

Detailed methods are provided in the online version of this paper and include the following:

- KEY RESOURCES TABLE
- EXPERIMENTAL MODEL AND STUDY PARTICIPANT DETAILS
- METHOD DETAILS
  - Animal collection and maintenance
  - Transcriptome sequencing and *de novo* assembly
  - *In silico* tyrosinase sequences identification
  - Protein extraction and mass spectrometry analyses
  - Localization of tyrosinase mRNA
  - Phylogenetic analyses and clustering analyses of tyrosinase sequences

SUPPLEMENTAL INFORMATION

Supplemental information can be found online at https://doi.org/10.1016/j.isci.2024.111443.

Received: July 19, 2024
Revised: October 13, 2024
Accepted: November 18, 2024
Published: November 20, 2024

REFERENCES

1. Delroisse, J., Kang, V., Gouveneaux, A., Santos, R., and Flammang, P. (2023). Convergent evolution of attachment mechanisms in aquatic animals. In Convergent Evolution. Fascinating Life Sciences, V.L. Bels and A.P. Russell, eds. (Springer). https://doi.org/10.1007/978-3-031-11441-0_16.
2. Almeida, M., Reis, R.L., and Silva, T.H. (2020). Marine invertebrates are a source of bioadhesives with biomimetic interest. Mater. Sci. Eng. C Mater. Biol. Appl. *108*, 110467. https://doi.org/10.1016/j.msec.2019.110467.
3. Li, X., Li, S., Huang, X., Chen, Y., Cheng, J., and Zhan, A. (2021). Protein-mediated bioadhesion in marine organisms : A review. Mar. Environ. Res. *170*, 105409. https://doi.org/10.1016/j.marenvres.2021.105409.
4. Hofman, A.H., van Hees, I.A., Yang, J., and Kamperman, M. (2018). Bio-inspired underwater adhesives by using the supramolecular toolbox. Adv. Mater. *30*, 1704640. https://doi.org/10.1002/adma.201704640.
5. Waite, J.H. (2017). Mussel adhesion – essential footwork. J. Exp. Biol. *220*, 517–530. https://doi.org/10.1242/jeb.134056.
6. Priemel, T., Degtyar, E., Dean, M.N., and Harrington, M.J. (2017). Rapid self-assembly of complex biomolecular architectures during mussel

byssus biofabrication. Nat. Commun. *8*, 14539. https://doi.org/10.1038/ncomms14539.

7. Vovelle, J. (1965). Le tube de *Sabellaria alveolata* (L.) : Annélide polychète Hermellidae et son ciment. Etude écologique, expérimentale, histologique et histochimique. Arch. Zool. Exp. Gen. *106*, 1–187.
8. Stewart, R.J., Weaver, J.C., Morse, D.E., and Waite, J.H. (2004). The tube cement of *Phragmatopoma californica*: a solid foam. J. Exp. Biol. *207*, 4727–4734. https://doi.org/10.1242/jeb.01330.
9. Becker, P.T., Lambert, A., Lejeune, A., Lanterbecq, D., and Flammang, P. (2012). Identification, characterization, and expression levels of putative adhesive proteins from the tube-dwelling polychaete *Sabellaria alveolata*. Biol. Bull. *223*, 217–225. https://doi.org/10.1086/BBLv223n2p217.
10. Wang, C.S., and Stewart, R.J. (2012). Localization of the bioadhesive precursors of the sandcastle worm, *Phragmatopoma californica* (Fewkes). J. Exp. Biol. *215*, 351–361. https://doi.org/10.1242/jeb.065011.
11. Stewart, R.J., Ransom, T.C., and Hlady, V. (2011). Natural underwater adhesives. J. Polym. Sci. B Polym. Phys. *49*, 757–771. https://doi.org/10.1002/polb.22256.
12. Petrone, L. (2013). Molecular surface chemistry in marine bioadhesion. Adv. Colloid Interface Sci. *195–196*, 1–18. https://doi.org/10.1016/j.cis.2013.03.006.
13. Davey, P.A., Power, A.M., Santos, R., Bertemes, P., Ladurner, P., Palmowski, P., Clarke, J., Flammang, P., Lengerer, B., Hennebert, E., et al. (2021). Omics-based molecular analyses of adhesion by aquatic invertebrates. Biol. Rev. *96*, 1051–1075. https://doi.org/10.1111/brv.12691.
14. Sagert, J., Sun, C., and waite, J.H. (2006). Chemical subtleties of mussel and polychaete holdfasts. In Biological adhesives (Springer Berlin Heidelberg), pp. 125–143.
15. Silverman, H.G., and Roberto, F.F. (2007). Understanding marine mussel adhesion. Mar. Biotechnol. *9*, 661–681. https://doi.org/10.1007/s10126-007-9053-x.
16. Priemel, T., Palia, R., Babych, M., Thibodeaux, C.J., Bourgault, S., and Harrington, M.J. (2020). Compartmentalized processing of catechols during mussel byssus fabrication determines the destiny of DOPA. Proc. Natl. Acad. Sci. USA *117*, 7613–7621. https://doi.org/10.1073/pnas.1919712117.
17. Laumer, C.E., Bekkouche, N., Kerbl, A., Goetz, F., Neves, R.C., Sørensen, M.V., Kristensen, R.M., Hejnol, A., Dunn, C.W., Giribet, G., and Worsaae, K. (2015). Spiralian phylogeny informs the evolution of microscopic lineages. Curr. Biol. *25*, 2000–2006. https://doi.org/10.1016/j.cub.2015.06.068.
18. Olivares, C., and Solano, F. (2009). New insights into the active site structure and catalytic mechanism of tyrosinase and its related proteins. Pigment Cell Melanoma Res. *22*, 750–760. https://doi.org/10.1111/j.1755-148X.2009.00636.x.
19. Aguilera, F., McDougall, C., and Degnan, B.M. (2013). Origin, evolution and classification of type-3 copper proteins: Lineage-specific gene expansions and losses across the Metazoa. BMC Evol. Biol. *13*, 96. https://doi.org/10.1186/1471-2148-13-96.
20. Ullrich, R., and Hofrichter, M. (2007). Enzymatic hydroxylation of aromatic compounds. Cellular and *Molecular Life Sciences*. Cell. Mol. Life Sci. *64*, 271–293. https://doi.org/10.1007/s00018-007-6362-1.
21. Ramsden, C.A., and Riley, P.A. (2014). Tyrosinase : The four oxidation states of the active site and their relevance to enzymatic activation, oxidation and inactivation. Bioorg. Med. Chem. *22*, 2388–2395. https://doi.org/10.1016/j.bmc.2014.02.048.
22. Del Marmol, V., and Beermann, F. (1996). Tyrosinase and related proteins in mammalian pigmentation. FEBS Lett. *381*, 165–168. https://doi.org/10.1016/0014-5793(96)00109-3.
23. Huan, P., Liu, G., Wang, H., and Liu, B. (2013). Identification of a tyrosinase gene potentially involved in early larval shell biogenesis of the Pacific oyster *Crassostrea gigas*. Dev. Genes Evol. *223*, 389–394. https://doi.org/10.1007/s00427-013-0450-z.
24. Sugumaran, M., Soderhall, K., Iwanaga, S., and Vastha, G. (1996). Role of insect cuticle in immunity. In New Directions in Invertebrate Immunology (SOS Publications), pp. 355–374.
25. Theopold, U., Schmidt, O., Söderhäll, K., and Dushay, M.S. (2004). Coagulation in arthropods : Defence, wound closure and healing. Trends Immunol. *25*, 289–294. https://doi.org/10.1016/j.it.2004.03.004.
26. González-Santoyo, I., and Córdoba-Aguilar, A. (2012). Phenoloxidase : A key component of the insect immune system: Biochemical and evolutionary ecology of PO. Entomol. Exp. Appl. *142*, 1–16. https://doi.org/10.1111/j.1570-7458.2011.01187.x.
27. Dennell, R. (1958). The hardening of insect cuticles. Biol. Rev. *33*, 178–196. https://doi.org/10.1111/j.1469-185X.1958.tb01306.x.
28. Andersen, S.O. (2010). Insect cuticular sclerotization: A review. Insect Biochem. Mol. Biol. *40*, 166–178. https://doi.org/10.1016/j.ibmb.2009.10.007.
29. Esposito, R., D'Aniello, S., Squarzoni, P., Pezzotti, M.R., Ristoratore, F., and Spagnuolo, A. (2012). New insights into the evolution of metazoan tyrosinase gene family. PLoS One *7*, e35731. https://doi.org/10.1371/journal.pone.0035731.
30. Waite, J.H. (1985). Catechol oxidase in the byssus of the common mussel, *Mytilus Edulis* L. J. Mar. Biol. Assoc. U. K. *65*, 359–371. https://doi.org/10.1017/S0025315400050487.
31. Hellio, C., Bourgougnon, N., and Gal, Y.L. (2000). Phenoloxidase (E.C. 1.14.18.1) from the byssus gland of *Mytilus edulis*: Purification, partial characterization and application for screening products with potential antifouling activities. Biofouling *16*, 235–244. https://doi.org/10.1080/08927010009378448.
32. Guerette, P.A., Hoon, S., Seow, Y., Raida, M., Masic, A., Wong, F.T., Ho, V.H.B., Kong, K.W., Demirel, M.C., Pena-Francesch, A., et al. (2013). Accelerating the design of biomimetic materials by integrating RNA-seq with proteomics and materials science. Nat. Biotechnol. *31*, 908–915. https://doi.org/10.1038/nbt.2671.
33. Qin, C.L., Pan, Q.D., Qi, Q., Fan, M.H., Sun, J.J., Li, N.N., and Liao, Z. (2016). In-depth proteomic analysis of the byssus from marine mussel *Mytilus coruscus. Journal of Proteomics*. J. Proteomics *144*, 87–98. https://doi.org/10.1016/j.jprot.2016.06.014.
34. Wang, C.S., and Stewart, R.J. (2013). Multipart copolyelectrolyte adhesive of the sandcastle worm, *Phragmatopoma californica* (Fewkes) : Catechol oxidase catalyzed curing through peptidyl-DOPA. Biomacromolecules *14*, 1607–1617. https://doi.org/10.1021/bm400251k.
35. Buffet, J.-P., Corre, E., Duvernois-Berthet, E., Fournier, J., and Lopez, P.J. (2018). Adhesive gland transcriptomics uncovers a diversity of genes involved in glue formation in marine tube-building polychaetes. Acta Biomater. *72*, 316–328. https://doi.org/10.1016/j.actbio.2018.03.037.
36. Endrizzi, B.J., and Stewart, R.J. (2009). Glueomics : An expression survey of the adhesive gland of the sandcastle worm. J. Adhes. *85*, 546–559. https://doi.org/10.1080/00218460902996457.
37. Flammang, P., Lambert, A., Bailly, P., and Hennebert, E. (2009). Polyphosphoprotein-containing marine adhesives. J. Adhes. *85*, 447–464. https://doi.org/10.1080/00218460902996358.
38. Kamino, K. (2010). Molecular design of barnacle cement in comparison with those of mussel and tubeworm. J. Adhes. *86*, 96–110. https://doi.org/10.1080/00218460903418139.
39. Frickey, T., and Lupas, A. (2004). CLANS: A Java application for visualizing protein families based on pairwise similarity. Bioinformatics *20*, 3702–3704. https://doi.org/10.1093/bioinformatics/bth444.
40. Pearson, W.R. (2013). An introduction to sequence similarity ("homology") searching. Curr. Protoc. Bioinformatics *Chapter 3*, 3.1.1–3.1.8. https://doi.org/10.1002/0471250953.bi0301s42.
41. Van Holde, K.E., and Miller, K.I. (1995). Hemocyanins. Adv. Protein Chem. *47*, 1–81. https://doi.org/10.1016/S0065-3233(08)60545-8.

42. Solomon, E.I., Sundaram, U.M., and Machonkin, T.E. (1996). Multicopper oxidases and oxygenases. Chem. Rev. *96*, 2563–2606. https://doi.org/10.1021/cr950046o.

43. Drexel, R., Siegmund, S., Schneider, H.-J., Linzen, B., Gielens, C., Préaux, G., Lontie, R., Kellermann, J., and Lottspeich, F. (1987). Complete amino-acid sequence of a functional unit from a molluscan hemocyanin (*Helix pomatia*). Biol. Chem. Hoppe Seyler *368*, 617–635. https://doi.org/10.1515/bchm3.1987.368.1.617.

44. Burmester, T., and Scheller, K. (1996). Common origin of arthropod tyrosinase, arthropod hemocyanin, insect hexamerin, and dipteran arylphorin receptor. J. Mol. Evol. *42*, 713–728. https://doi.org/10.1007/BF02338804.

45. Aguilera, F., McDougall, C., and Degnan, B.M. (2014). Evolution of the tyrosinase gene family in bivalve molluscs: Independent expansion of the mantle gene repertoire. Acta Biomater. *10*, 3855–3865. https://doi.org/10.1016/j.actbio.2014.03.031.

46. Waite, J.H. (1990). The phylogeny and chemical diversity of quinone-tanned glues and varnishes. Comp. Biochem. Physiol. B *97*, 19–29. https://doi.org/10.1016/0305-0491(90)90172-P.

47. DeMartini, D.G., Errico, J.M., Sjoestroem, S., Fenster, A., and Waite, J.H. (2017). A cohort of new adhesive proteins identified from transcriptomic analysis of mussel foot glands. J. R. Soc. Interface *14*, 20170151. https://doi.org/10.1098/rsif.2017.0151.

48. Papov, V.V., Diamond, T.V., Biemann, K., and Waite, J.H. (1995). Hydroxyarginine-containing polyphenolic proteins in the adhesive plaques of the marine mussel *Mytilus edulis*. J. Biol. Chem. *270*, 20183–20192. https://doi.org/10.1074/jbc.270.34.20183.

49. Waite, J.H., and Qin, X. (2001). Polyphosphoprotein from the adhesive pads of *Mytilus edulis*. Biochemistry *40*, 2887–2893. https://doi.org/10.1021/bi002718x.

50. Waite, J.H., and Tanzer, M.L. (1981). Polyphenolic substance of *Mytilus edulis* : Novel adhesive containing L-dopa and hydroxyproline. Science *212*, 1038–1040. https://doi.org/10.1126/science.212.4498.1038.

51. Qin, X.-X., Coyne, K.J., and Waite, J.H. (1997). Tough tendons. Mussel byssus has collagen with silk-like domains. J. Biol. Chem. *272*, 32623–32627. https://doi.org/10.1074/jbc.272.51.32623.

52. Sagert, J., and Waite, J.H. (2009). Hyperunstable matrix proteins in the byssus of *Mytilus galloprovincialis*. J. Exp. Biol. *212*, 2224–2236.

53. Waite, J.H., Jensen, R.A., and Morse, D.E. (1992). Cement precursor proteins of the reef-building polychaete *Phragmatopoma californica* (Fewkes). Biochemistry *31*, 5733–5738. https://doi.org/10.1021/bi00140a007.

54. Pretzler, M., and Rompel, A. (2018). What causes the different functionality in type-III-copper enzymes? A state of the art perspective. Inorg. Chim. Acta. *481*, 25–31. https://doi.org/10.1016/j.ica.2017.04.041.

55. Jaenicke, E., and Decker, H. (2003). Tyrosinases from crustaceans form hexamers. Biochem. J. *371*, 515–523. https://doi.org/10.1042/bj20021058.

56. Lee, B.P., Messersmith, P.B., Israelachvili, J.N., and Waite, J.H. (2011). Mussel-inspired adhesives and coatings. Annu. Rev. Mater. Res. *41*, 99–132. https://doi.org/10.1146/annurev-matsci-062910-100429.

57. Schmitt, C.N.Z., Winter, A., Bertinetti, L., Masic, A., Strauch, P., and Harrington, M.J. (2015). Mechanical homeostasis of a DOPA-enriched biological coating from mussels in response to metal variation. J. R. Soc. Interface *12*, 20150466. https://doi.org/10.1098/rsif.2015.0466.

58. Yu, J., Wei, W., Danner, E., Ashley, R.K., Israelachvili, J.N., and Waite, J.H. (2011). Mussel protein adhesion depends on interprotein thiol-mediated redox modulation. Nat. Chem. Biol. *7*, 588–590. https://doi.org/10.1038/nchembio.630.

59. Wang, J., Suhre, M.H., and Scheibel, T. (2019). A mussel polyphenol oxidase-like protein shows thiol-mediated antioxidant activity. Eur. Polym. J. *113*, 305–312. https://doi.org/10.1016/j.eurpolymj.2019.01.069.

60. Zhao, H., Sun, C., Stewart, R.J., and Waite, J.H. (2005). Cement proteins of the tube-building polychaete *Phragmatopoma californica*. J. Biol. Chem. *280*, 42938–42944. https://doi.org/10.1074/jbc.M508457200.

61. Sun, J., Han, J., Wang, F., Liu, K., and Zhang, H. (2022). Bioengineered protein-based adhesives for biomedical applications. Chem. Eur J. *28*, e202102902. https://doi.org/10.1002/chem.202102902.

62. Lutz, T.M., Kimna, C., Casini, A., and Lieleg, O. (2022). Bio-based and bio-inspired adhesives from animals and plants for biomedical applications. Mater. Today. Bio *13*, 100203. https://doi.org/10.1016/j.mtbio.2022.100203.

63. Wang, J., and Scheibel, T. (2018). Recombinant production of mussel byssus inspired proteins. Biotechnol. J. *13*, 1800146. https://doi.org/10.1002/biot.201800146.

64. Harrington, M.J., Jehle, F., and Priemel, T. (2018). Mussel byssus structure-function and fabrication as inspiration for biotechnological production of advanced materials. Biotechnol. J. *13*, 1800133. https://doi.org/10.1002/biot.201800133.

65. Kitamura, M., Kawakami, K., Nakamura, N., Tsumoto, K., Uchiyama, H., Ueda, Y., Kumagai, I., and Nakaya, T. (1999). Expression of a model peptide of a marine mussel adhesive protein in *Escherichia coli* and characterization of its structural and functional properties. J. Polym. Sci. A. Polym. Chem. *37*, 729–736. https://doi.org/10.1002/(SICI)1099-0518(19990315)37:6<729::AID-POLA8>3.0.CO;2-3.

66. Hwang, D.S., Yoo, H.J., Jun, J.H., Moon, W.K., and Cha, H.J. (2004). Expression of functional recombinant mussel adhesive protein Mgfp-5 in *Escherichia coli*. Appl. Environ. Microbiol. *70*, 3352–3359. https://doi.org/10.1128/AEM.70.6.3352-3359.2004.

67. Choi, Y.S., Yang, Y.J., Yang, B., and Cha, H.J. (2012). In vivo modification of tyrosine residues in recombinant mussel adhesive protein by tyrosinase co-expression in *Escherichia coli*. Microb. Cell Fact. *11*, 139. https://doi.org/10.1186/1475-2859-11-139.

68. Yao, L., Wang, X., Xue, R., Xu, H., Wang, R., Zhang, L., and Li, S. (2022). Comparative analysis of mussel foot protein 3B co-expressed with tyrosinases provides a potential adhesive biomaterial. Int. J. Biol. Macromol. *195*, 229–236. https://doi.org/10.1016/j.ijbiomac.2021.11.208.

69. Grabherr, M.G., Haas, B.J., Yassour, M., Levin, J.Z., Thompson, D.A., Amit, I., Adiconis, X., Fan, L., Raychowdhury, R., Zeng, Q., et al. (2011). Full-length transcriptome assembly from RNA-Seq data without a reference genome. Nat. Biotechnol. *29*, 644–652. https://doi.org/10.1038/nbt.1883.

70. Waterhouse, R.M., Seppey, M., Simão, F.A., Manni, M., Ioannidis, P., Klioutchnikov, G., Kriventseva, E.V., and Zdobnov, E.M. (2018). BUSCO applications from quality assessments to gene prediction and phylogenomics. Mol. Biol. Evol. *35*, 543–548. https://doi.org/10.1093/molbev/msx319.

71. Paysan-Lafosse, T., Blum, M., Chuguransky, S., Grego, T., Pinto, B.L., Salazar, G.A., Bileschi, M.L., Bork, P., Bridge, A., Colwell, L., et al. (2023). InterPro in 2022. Nucleic Acids Res. *51*, D418–D427. https://doi.org/10.1093/nar/gkac993.

72. Teufel, F., Almagro Armenteros, J.J., Johansen, A.R., Gíslason, M.H., Pihl, S.I., Tsirigos, K.D., Winther, O., Brunak, S., Von Heijne, G., and Nielsen, H. (2022). SignalP 6.0 predicts all five types of signal peptides using protein language models. Nat. Biotechnol. *40*, 1023–1025. https://doi.org/10.1038/s41587-021-01156-3.

73. Katoh, K., Rozewicki, J., and Yamada, K.D. (2019). MAFFT online service : Multiple sequence alignment, interactive sequence choice and visualization. Brief. Bioinform. *20*, 1160–1166. https://doi.org/10.1093/bib/bbx108.

74. Capella-Gutierrez, S., Silla-Martinez, J.M., and Gabaldon, T. (2009). trimAl: A tool for automated alignment trimming in large-scale phylogenetic analyses. Bioinformatics *25*, 1972–1973. https://doi.org/10.1093/bioinformatics/btp348.

75. Hoang, D.T., Chernomor, O., Von Haeseler, A., Minh, B.Q., and Vinh, L.S. (2018). UFBoot2 : Improving the ultrafast bootstrap approximation. Mol. Biol. Evol. *35*, 518–522. https://doi.org/10.1093/molbev/msx281.

76. Trifinopoulos, J., Nguyen, L.-T., von Haeseler, A., and Minh, B.Q. (2016). W-IQ-TREE : A fast online phylogenetic tool for maximum likelihood

analysis. Nucleic Acids Res. *44*, W232–W235. https://doi.org/10.1093/nar/gkw256.

77. Letunic, I., and Bork, P. (2021). Interactive Tree Of Life (iTOL) v5 : An online tool for phylogenetic tree display and annotation. Nucleic Acids Res. *49*, W293–W296. https://doi.org/10.1093/nar/gkab301.
78. Tamarin, A., Lewis, P., and Askey, J. (1976). The structure and formation of the byssus attachment plaque in *Mytilus*. J. Morphol. *149*, 199–221. https://doi.org/10.1002/jmor.1051490205.
79. Rzepecki, L.M., Hansen, K.M., and Waite, J.H. (1992). Characterization of a cystine-rich polyphenolic protein family from the blue mussel *Mytilus edulis* L. Biol. Bull. *183*, 123–137. https://doi.org/10.2307/1542413.
80. Jensen, R.A., and Morse, D.E. (1988). The bioadhesive of *Phragmatopoma californica* tubes: a silk-like cement containing L-DOPA. J. Comp. Physiol. B *158*, 317–324. https://doi.org/10.1007/BF00695330.
81. Hennebert, E., Leroy, B., Wattiez, R., and Ladurner, P. (2015). An integrated transcriptomic and proteomic analysis of sea star epidermal secretions identifies proteins involved in defense and adhesion. J. Proteomics *128*, 83–91. https://doi.org/10.1016/j.jprot.2015.07.002.
82. Lengerer, B., Wunderer, J., Pjeta, R., Carta, G., Kao, D., Aboobaker, A., Beisel, C., Berezikov, E., Salvenmoser, W., and Ladurner, P. (2018). Organ specific gene expression in the regenerating tail of Macrostomum lignano. Dev. Biol. *433*, 448–460. https://doi.org/10.1016/j.ydbio.2017.07.021.
83. Pfister, D., De Mulder, K., Philipp, I., Kuales, G., Hrouda, M., Eichberger, P., Borgonie, G., Hartenstein, V., and Ladurner, P. (2007). The exceptional stem cell system of *Macrostomum lignano* : Screening for gene expression and studying cell proliferation by hydroxyurea treatment and irradiation. Front. Zool. *4*, 9. https://doi.org/10.1186/1742-9994-4-9.

STAR★METHODS

KEY RESOURCES TABLE

REAGENT or RESOURCE	SOURCE	IDENTIFIER
Antibodies		
Antidigoxigenin-AP Fab fragments (Roche, USA)	Sigma Aldrich, USA	11093274910; RRID: AB_2734716
Chemicals, peptides, and recombinant proteins		
TRIzol Reagent	ThermoFisher, USA	15596026
Sera-Mag Magnetic Oligo(dT)-coated beads	Illumina, USA	N/A
DIG RNA Labeling Mix (Roche, USA)	Sigma Aldrich, USA	11277073910
T7 RNA polymerase	Promega, USA	P2075
NBT/BCIP system (Roche, USA)	Sigma Aldrich, USA	11681451001
Critical commercial assays		
Truseq Stranded mRNA Sample Preparation kit	Illumina, USA	N/A
Non-Interfering Protein Assay Kit	Calbiochem, Germany	N/A
RC DC Protein Assay Kit I	BioRad, USA	5000121
2-D Clean-Up Kit	GE Healthcare, USA	N/A
Reverse transcription kit	Roche, USA	N/A
Q5 High-Fidelity DNA Polymerase kit	New England Biolabs, UK	M0491L
Wizard SV Gel and PCR clean-up system kit	Promega, USA	A9281
Deposited data		
Raw sequencing data of the transcriptome of the foot of *M. edulis* (Sequence Read Archive)	NCBI, USA (https://www.ncbi.nlm.nih.gov/sra)	NCBI SRA: SRR29446349
Raw sequencing data of the transcriptome of the anterior part of *S. alveolata* (Sequence Read Archive)	NCBI, USA (https://www.ncbi.nlm.nih.gov/sra)	NCBI SRA: SRR29446350
Experimental models: Organisms/strains		
Mytilus edulis Linnaeus, 1758 (Mollusca)	Collected by authors	N/A
Sabellaria alveolata (Linnaeus, 1767) (Annelida)	Station Biologique de Roscoff, France	N/A
Oligonucleotides		
Primers used to generate *in situ* hybridization probes	Sigma-Aldrich, USA	See Table S2
Software and algorithms		
FastQC software	Babraham Bioinformatics, UK	https://www.bioinformatics.babraham.ac.uk/projects/
Trinity software	Grabherr et al., 2011[69]	N/A
BUSCO software, v3.0.2	Waterhouse et al., 2018[70]	https://gitlab.com/ezlab/busco
BLAST online tool	NCBI, USA	https://blast.ncbi.nlm.nih.gov/Blast.cgi
ExPASY Translate online tool	SIB (Swiss Institute of Bioinformatics)	https://web.expasy.org/translate/
InterPro online tool	Paysan-Lafosse et al., 2023[71]	https://www.ebi.ac.uk/interpro/search/sequence/
SignalP-6.0 online tool	Teufel et al., 2022[72]	https://services.healthtech.dtu.dk/service.php?SignalP
Protein Pilot software, v5.0.1	Sciex, US	https://sciex.com/products/software/proteinpilot-software
MaxQuant software, v1.4.1.2	Cox lab	https://www.maxquant.org/
Open Primer 3 online tool	ELIXIR (European research infrastructure for biological information, EE)	https://bioinfo.ut.ee/primer3/
CLANS (Cluster analysis of sequences) software	Frickey & Lupas, 2004[39]	https://toolkit.tuebingen.mpg.de/clans/

(*Continued on next page*)

Continued

REAGENT or RESOURCE	SOURCE	IDENTIFIER
MAFFT software, v7.490 (implemented in the Geneious Prime software, v2.1)	Katoh et al., 2019, Geneious Prime[73]	www.geneious.com
TrimAL software (implemented in the Phylemon2 online tool)	Capella-Gutierrez et al., 2009[74]	http://phylemon.bioinfo.cipf.es/
IQTREE software, v1.6.12	Hoang et al., 2018[75]	http://www.iqtree.org/
MEGA software, v10	Trifinopoulos et al., 2016[76]	https://www.megasoftware.net/dload_win_gui
iTOL (Interactive Tree of Life) online tool, v6.9	Letunic & Bork, 2021[77]	https://itol.embl.de/
Other		
Glass beads, unwashed (425-600 μm in diameter)	Sigma Aldrich	G9268-100G

EXPERIMENTAL MODEL AND STUDY PARTICIPANT DETAILS

Our experimental models included adult individuals of the blue mussel *Mytilus edulis* Linnaeus, 1758 (Mollusca, Bivalvia) and of the honeycomb worm *Sabellaria alveolata* Linnaeus, 1767 (Annelida, Polychaeta). The sex of the individuals was not determined. Neither of these species is threatened and no permits are required for their collection or maintenance. The authors have complied with all ethical standards required for conducting this research and the animals used in the experiments were maintained and treated in compliance with the guidelines specified by the Belgian Ministry of Trade and Agriculture.

METHOD DETAILS

Animal collection and maintenance

Individuals of *Mytilus edulis* were collected intertidally in Audresselles (Pas-de-Calais, France). Reef fragments of *Sabellaria alveolata* were collected at low tide on the ''plage de Ris'' at Douarnenez, France (48°05'34.6''N 4°17'55.0''W), or were obtained from the Station Biologique de Roscoff (Finistere, France). All animals were then transported to the Laboratory of Biology of Marine Organisms and Biomimetics (University of Mons, Belgium), where they were kept in a re-circulating aquarium (13°C, 33 psu salinity).

Transcriptome sequencing and *de novo* assembly

In the present study, two tissue transcriptomes have been generated: one from the foot of the blue mussel *M. edulis* and one from the anterior part of the honeycomb worm *S. alveolata*.

RNA extraction, library construction and sequencing were performed at the GIGA Genomics platform (Liège, Belgium). After dissection, mussel feet and tubeworm anterior parts (corresponding to the head and parathoracic region) were immediately frozen with liquid nitrogen and stored at -80°C until use. Total RNA was extracted from 100 mg of frozen tissue using Trizol (Life Technologies, Carlsbad, CA) and its quality was assessed using the Bioanalyser 2100 (Agilent). Truseq Stranded mRNA Sample Preparation kit (San Diego, CA) was used to prepare a library from 500 ng of total RNA. Poly-adenylated RNAs were purified with oligo (dT)-coated magnetic beads (Sera-Mag Magnetic Oligo(dT) beads, Illumina) and then chemically fragmented to a length of 100 to 400 nucleotides -with a majority of the fragments at about 200 bp (base pairs)- by using divalent cations at 94°C for 5 min. These short fragments were used as a template for reverse-transcription using random hexamers to synthesise cDNA, followed by end repair and adaptor ligation according to the manufacturer's protocol (Illumina, San Diego, CA). Finally, the ligated library fragments were purified and enriched by solid-phase PCR following Illumina's protocol. The library quality was validated on the Bioanalyser 2100. The high-throughput sequencing was conducted by a HiSeq 2000 platform (Illumina, San Diego, CA) to obtain 2x100-bp paired-end reads according to manufacturer's instructions. Real-time quality control was performed to ensure that most read quality score was higher than 30. The raw sequencing data have been deposited in the NCBI Sequence Read Archive with accession numbers NCBI SRA: SRR29446349 and NCBI SRA: SRR29446350 for *M. edulis* and *S. alveolata*, respectively.

Transcriptome quality was checked using Fast QC software (Babraham Bioinformatics). The Trinity software suite[69] which comprises a quality filtering function was used with default parameters to *de novo* assemble the raw reads with overlapping nucleic acid sequence into contigs. Transcriptome completeness was evaluated using BUSCO (v3.0.2) analyses on assembled transcripts.[70] Scores were calculated using Metazoan_odb10 lineage data.

In silico tyrosinase sequences identification

To find the tyrosinase sequences putatively involved in adhesive protein maturation, tBLASTn searches were performed on the two transcriptomes using a reference dataset (see Table S1) consisting of byssus-specific tyrosinase sequences found in *M. coruscus*[33] and *P. viridis*[32] and of a cement tyrosinase sequence from the tubeworm *P. californica*.[10] Several transcripts encoding tyrosinase-like

proteins were obtained for both species. They were subsequently used in a reciprocal tBLASTn search against the NCBI non-redundant protein database and only those having a tyrosinase as the best-hit match were kept for further analyses.

The selected transcripts were translated *in silico* (Expasy, Translate tool) and analyzed by looking for the tyrosinase copper-binding domain (IPR002227) using InterPro (https://www.ebi.ac.uk/interpro/search/sequence/)[71] and for the presence of a signal peptide using SignalP-6.0 (https://services.healthtech.dtu.dk/service.php?SignalP).[72]

Protein extraction and mass spectrometry analyses

To assess whether tyrosinase enzymes are secreted in the adhesive materials of mussels and tubeworms, proteomic analyses were conducted on induced byssal threads and reconstructed tubes.

For *M. edulis*, the secretion of fresh byssal threads was induced by injecting a 0.56 M solution of KCl at the base of the foot as described by Tamarin et al.[78] For protein extraction, approximately 30 byssal threads were crushed in 500 μL of a solution containing 5% acetic acid and 8 M urea.[79] The extract was then centrifuged for 20 min at 16,000g and the supernatant containing the proteins was collected. For *S. alveolata*, single tubes with their dwelling worm were isolated from the reef fragment. The upper third of each tube was then removed and the worms were allowed to reconstruct this missing portion of their tube with glass beads (425-600 μm in diameter; Sigma).[80] Approximately 500 mg of freshly rebuilt tube fragments were subjected to protein extraction using a 1.5 M Tris–HCl buffer (pH 8.5) containing 7 M guanidine hydrochloride (GuHCl), 20 mM ethylenediaminetetraacetate (EDTA), and 0.5 M dithiothreitol (DTT) (Tris-GuHCl buffer). This mixture was incubated for 1 hour at 60°C under agitation and then centrifuged as described above.

To further process proteins, both samples were treated with a 2.5-fold excess (w/w) of iodoacetamide to DTT, for 20 min in the dark at room temperature, to carbamidomethylate the sulfhydryl groups. The reaction was then stopped by adding an equal quantity of β-mercaptoethanol to iodoacetamide. The extract was centrifuged at 13,000 rpm for 15 min at 4°C and the supernatant was collected. The protein concentration was determined using the Non-Interfering Protein Assay Kit (Calbiochem, Darmstadt, Germany) with bovine serum albumin as a protein standard. For each sample, 50 μg of proteins were then precipitated overnight at -20°C in 80% acetone. After a 15-min centrifugation at 13,000 rpm and evaporation of acetone, the resulting pellet was subjected to overnight enzymatic digestion using modified porcine trypsin at an enzyme/substrate ratio of 1/50, at 37°C in 25 mM NH_4HCO_3. The reaction was stopped by adding formic acid to a final concentration of 0.1% (v/v).[81] Tryptic peptides were analysed by LC connected to a hybrid quadrupole time-of-flight TripleTOF 6600 mass spectrometer (AB SCIEX, Concord, ON). Byssal threads and reconstructed tubes MS/MS data were searched for protein candidates against a database composed of the six open reading frames (ORFs) of the transcriptome of the foot of *M. edulis* or of the transcriptome of the anterior part of *S. alveolata*, respectively, using the Protein Pilot software (version 5.0.1). The samples with a false discovery rate (FDR) above 1.0% were excluded from subsequent analyses.

A proteomic analysis was also carried out on the mussel foot tissues. Feet were dissected and cut transversely into two halves to separate the proximal part from the distal part. The samples were homogenized in a Potter-Elvehjem tissue grinder with a 4% solution of SDS in Tris-HCl buffer (pH 7.4), with protease inhibitors (EDTA-free), and 5 units of DNase per 100 mg of foot tissue. The samples were then sonicated three times for 30 s each and left at room temperature for 30 min, followed by overnight incubation at 4°C. The protein content was quantified using an RCDC kit (Biorad). Aliquots of 15 μg of proteins were reduced and alkylated. The samples were then treated with the 2-D Clean-Up Kit (GE Healthcare) to eliminate impurities not compatible with mass spectrometry analyses and recovered in 50 mM ammonium bicarbonate buffer. Trypsin digestion was carried out for 16 hours at an enzyme/substrate ratio of 1/50 at 37°C, the reaction was stopped by adding trifluoroacetic acid, and the samples were dried using a speed vac. The tryptic peptides were dissolved in water with 0.1% trifluoroacetic acid and purified using a Zip-Tip C18 High Capacity. They were analysed by reverse-phase HPLC–ESI-MS/MS using a nano-UPLC (nanoAcquity, Waters) connected to an ESI-Q-Orbitrap mass spectrometer (Q Extractive Thermo) in positive ion mode. MS/MS data were analysed against a database composed of the six open reading frames (ORFs) of the mussel foot transcriptome using the MaxQuant software (version 1.4.1.2). The peptide mass tolerance was set to ±10 ppm, and fragment mass tolerance was set to ±0.1 Da. The oxidation of the amino acids tyrosine, arginine and proline, as well as the carbamidomethylation of cysteine and the phosphorylation of serine were defined as fixed modifications, and the oxidation of methionine as variable modifications. Protein identifications were considered significant if proteins are identified with at least two peptides per protein taking into account only an FDR<0.01.

Localization of tyrosinase mRNA

The best tyrosinase sequence candidates found in the *in silico* and proteomic analyses were localized using *in situ* hybridization (ISH) technique to see if they are well expressed in the adhesive glands of both studied species. RNA was extracted from three parathoracic parts of honeycomb worms and three blue mussel feet using TRIzol™ Reagent kit (Thermofisher). The cDNA synthesis from the RNA extracted was done using Reverse transcription kit, Roche. Later, double-stranded DNA templates were amplified by PCR using the Q5 High-Fidelity DNA Polymerase kit method, with primer designed by Open Primer 3 (bioinfo.ut.ee/primer3/) with an optimal probe length between 700 and 900 bp. A second PCR was done with T7 promoter binding site (5'-GGATCCTAATACGACTCACTA TAGG-3') added to reverse strand PCR primers. PCR products were purified using the Wizard SV Gel and PCR clean-up system kit (Promega) and used for RNA probe synthesis. Digoxigenin (DIG)-labelled RNA probes were then synthesized with the kit DIG RNA Labelling Kit (Roche) with T7 RNA polymerase and DIG–dUTP. *In situ* hybridization was performed according to Lengerer et al., 2018.[82] The probes were used on parathoracic sections showing the adhesive glands for the honeycomb worm, and transversal

sections of the blue mussel foot, at a concentration of 0.2ng/μl and detected with antidigoxigenin-AP Fab fragments (Roche) at a dilution of 1:2000. The signal was developed using the NBT/BCIP system (Roche) at a dilution of 1:50 at 37°C. Sections were observed using a Zeiss Axioscope A1 microscope connected to a Zeiss AxioCam 305 color camera.

To confirm the localization of the candidates in the blue mussel, we conducted a complementary whole mount *in situ* hybridization. For each candidate, the mussel feet were divided into two parts along the frontal axis. The protocol was done in 6-well plates according to Pfister et al., 2007,[83] except for these steps; the *in situ* hybridization was carried out on samples re-incubated at 55°C for 72 hours, and color development was performed in the dark at 37°C using an NBT/BCIP system (Roth) until a satisfactory precipitate coloration was achieved.

Phylogenetic analyses and clustering analyses of tyrosinase sequences

To gain a deeper understanding of the relationship between all the tyrosinase enzymes, we conducted a CLANS analysis on a comprehensive dataset. This dataset included lophotrochozoan sequences in FASTA format, each containing a pfam00264 domain. These sequences were retrieved from the NCBI database (retrieved on September 20, 2022). In addition, we also incorporated the previously identified sequences obtained through *in silico* and proteomic analyses. We also incorporated three tyrosinase transcripts from the transcriptome of *Mytilus edulis*, which exhibited higher expression levels in mantle tissues (Matthew J. Harrington personal communication). To expand the diversity of tubeworm tyrosinases within the phylum Annelida, we obtained transcriptomes from *Phragmatopoma caudata*.[35] We conducted a local tBLASTn search targeting tyrosinase mRNA sequences that may play a role in protein cement maturation, using the previously mentioned *P. californica* sequence. As the number of sequences was relatively limited for Annelida compared with other phyla, we conducted a complementary analysis. In this analysis, we searched for the pfam00264 domain among the sequences found in the transcriptomes of *Capitella teleta* (3 transcripts), *Owenia fusiformis* (13 transcripts), *Oasisia alvinae* (4 transcripts), and *Riftia pachyptila* (3 transcripts), all of which are available on https://github.com/ChemaMD. The CLANS analysis was based on all-against-all sequence similarity using BLAST searches with the BLOSUM62 matrix (https://toolkit.tuebingen.mpg.de/clans/).[39]

We performed a phylogenetic analysis using the tyrosinase sequences from two closely clustered groups identified in the CLANS analysis, and which contained the sequences from the two studied species. First, we conducted a multiple alignment with all these sequences, totaling 312 sequences, using the MAFFT algorithm (using the automated parameters of Mafft v7.490 implemented on Geneious Prime 2023.2.1[73]). Subsequently, we trimmed this alignment using the online TrimAL tool implemented on Phylemon2[74] with the Automated1 option parameter. We selected two tyrosinase sequences from Mollusca, which contained a hemocyanin domain as outgroup. The construction of the phylogenetic tree was carried out using the IQ-TREE (1.6.12) software, using the maximum likelihood method and performing ultrafast bootstrap (UFBoot) analysis with 1000 replicates.[75] According to the software's BIC scores, the best-fit model was determined to be the WAG+F+I+G4 model.[76] The tree was modified using the software iTOL (version 6.9).[77]